Measurements of Lesser sandeel schools (*Ammodytes marinus*) using omnidirectional fisheries sonar

Master thesis of Fisheries Biology and Management

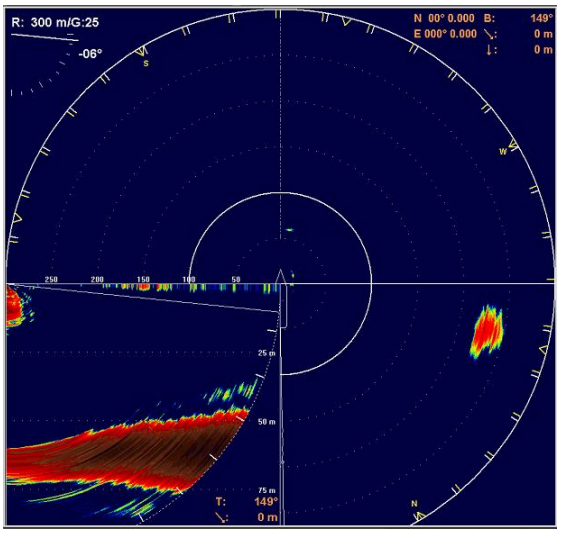

Student: Didrik Vartdal

Supervisor: Egil Ona

UNIVERSITY OF BERGEN
FACULTY OF MATHEMATICS AND NATURAL SCIENCE
BIOLOGY DEPARTMENT

August, 2012

CONTENT

ABSTRACT

The coverage of this master thesis is 58 pages, with 25 Figures and 9 Tables.

The Simrad SH90 high frequency omidirectional sonar was used in a field experiment in 2011 to acoustically investigate the distribution of Lesser sandeel (*Ammodytes marinus*) during the North Sea sandeel survey by the Norwegian research vessel "Johan Hjort". The sonar was applied together with conventional echo sounder survey, with trawl and dredge sample stations at various point. During the survey, sonar screenshots were recorded for 750 school from the total survey period, while two sandeel banks, the "Inner Shoal East" and "Hardangervidda" was investigated by using post-processing software LSSS for echo sounder data and PROFOS for sonar data. Sandeel school parameters were carefully analyzed from the screenshots by using the image editing software "ImageJ".

The results show that sandeel schools can well be detected with the Simrad SH90 omnidirectional sonar in good to fair weather conditions. The effective detection range for weak schools in shallow water is about 250 m. The sonar showed greater capability of detecting sandeel schools during a conventional acoustic survey, with 3.02 and 1.44 times the detections of the echo sounder for Inner Shoal East and Hardangervidda respectively. The school area, perimeter, shape and position relative to the vessel, show that sandeel schools are relative large with an average horizontal area of 1225 m^2. However, the sonar system showed detection limitations with respect to the smaller schools situated near the seabed. A comparisons made between sandeel schools detected with both acoustic systems, show that the relative size of smaller sandeel schools are more often underestimated in areal size compared with the sonar, while the larger schools are overestimated. The sonar survey show examples of potential missing of schools on echo sounder transects, and have therfore the potential for being a good tool in future two stage adaptive surveys.

INTRODUCTION

Recently it has been shown (Johnsen *et al*. 2009; Kubelius, 2009) that it is possible to measure the acoustic characteristics of sandeel in the water column during daytime, and that the total biomass within beds or specific sandeel grounds can be measured acoustically. However several aspects of the sandeel biology and swimming behaviour may restrict the applicability of acoustic survey methodology. Besides target strength, species indentification, sandeel burrowing behaviour and school distribution across the sandeel bed, the small relative volume sampled by a traditional echo sounder beam is viewed as one of the largest challenges with respect to the total uncertainty of the sandeel abundance estimate.

Sandeel is a small fish without a swimbladder (Winslade, 1974) that gives a relatively weak backscatter on the echogram. When schooling, it can be detected by both echo sounders and fisheries sonar, but with a lower intensity compared to swimbladdered species such as herring (Clupea harengus). While the detection and abundance estimation is best conducted by echo sounders, it is believed that omnidirectional sonar may be used to study the school patchiness and areal distribution of sandeel schools. Both subjects are relevant in a survey design. This assignment will discuss the results after an experimental survey with a high frequency fisheries omnidirectional sonar (SH90) for detection of sandeel schools. The expected results were to give an evaluation of the sonar's school detection ability and compare it with echo sounder detections, knowledge of sandeel school distribution, size and shape from the sonar areal coverage during surveying.

Several assumptions were considered in advance, before conducting the experiment. Sandeel schools are normally distributed in "patches" across the North Sea fishing grounds and the estimate of mean density may have high uncertainty. Instead of increasing the survey effort by increased degree of coverage (DC), higher coverage can be more efficiently achieved by increasing the acoustic sampling volume. It was expected that the sonar could detect large and tall schools quite well, while smaller schools or patches located close to the seabed would have a significantly lower detection probability. The sonars detection probability could aslo be affected by rough weather or by variable bottom hardness, creating noise that conceal targets on the sonar display.

The survey was conducted by the Norwegian Institute of Marine Research (IMR) by the scientific vessel Johan Hjort. Sonar data was collected south of the Norwegian shore in the North Sea during march and may 2011. The primary objective of the survey was to measure sandeel abundance with the EK60 echo sounder in order to give a scientific advice regarding

the foregoing year's sandeel fisheries quota. Johan Hjort had however recently aquired the newly developed Simrad SH90 sonar that was installed prior to the survey for trials spesific on sandeel schools.

The objective of this thesis is:

1. Can sandeel schools be detected with the sonar?
2. What is the effective detection range of the sonar under the prevailing hydrographic conditions?
3. Is it possible to quantify the school size and shape with the sonar?
4. Does the echo sounder and sonar detect the areal distribution of schools similarly on the field?

1. LITTERATURE REVIEW

1.1 Biology and ecology of lesser sandeel (*Ammodytes marinus*)

There exists seven different species of sandeels in the North Sea, were the Lesser sandeel (*Ammodytes marinus*) is the most common species. Sandeels are a schooling fish which usually occur in coastal and shallow open-ocean waters, but also sometimes in depths of 200 m. Lesser sandeel is widely distributed throughout the North Sea region and occur in large numbers along the coast as far as the Kola Peninsula. It is also possible to find the species near the Faroe Islands, Iceland, Greenland and far east in the Baltic Sea around Bornholm. (Winslade, 1974). Sandeel constitute an important prey for many top predators and commercial fish species, such as cod (*Gadus morhua*), haddock (*Melanogrammus aeglefinus*), whiting (*Merlangius merlangus*), saithe (*Pollachiusvirens*), mackerel (*Scomber scombrus*) as well as many sea birds (Greenstreet *et al.*, 2006).

Sandeel are today harvested industrially at a large scale by, mainly because of their high quality oil content that is used in the production of fishmeal. It's therefore relevant to gain more knowledge about the current state of the population in our waters (Hassel *et al*., 2004) The North Sea's fishing fleet delivers the catch to factories where it is converted in to fishmeal and further used in the production of feed for aquaculture farms. It is possible to use sandeel for human consumption but not particular common (Greenstreet *et al.*, 2006). Fisheries biologists have been concerned about the sustainability of the sandeel population after a stock collapse in 2003 due to overfishing of the spawing stock biomass during the nineties. In 2010, ICES in cooperation with IMR accomplished a thorough assessment of

sandeel populations in the North Sea. (ICES, 2010) These estimations were used to set the 2011 quotas of sandeel for future sustainable populations in the North Sea. The critical harvest limit where set at 320 000 tons which included all fishing grounds for ICES members (ICES, 2011). This quota is quite below the amount compared to the North Sea landings during the nineties, which averaged with around 815 000 tons each year (Johannessen, 2009).

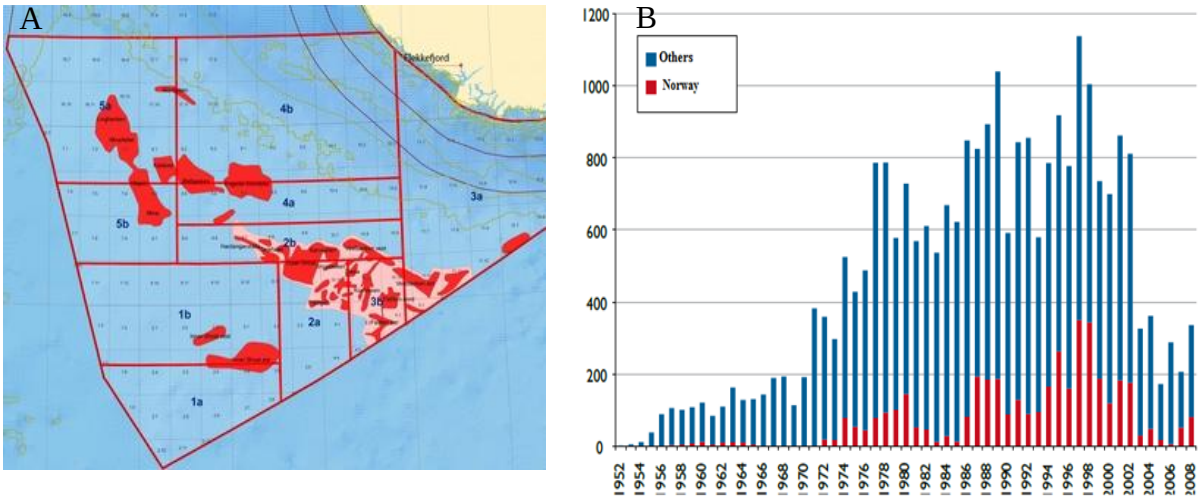

Figure 1. A) Most important sandeel distribution areas in the Norwegian Economical Zone. B) Total landings of sandeel by norwegian fishing fleet and other countries during the period 1952 to 2008. (Image from Johannesen, 2009)

The latest management model for sandeel fisheries implements an advanced stage of marine protected areas (MPA), where parts of the fishing areas are closed down during a fisheries season while they subsequently switch availability with each other the next year. The goal is to maintain a sustainable local breeding population in the whole natural habitat of the sandeel. This may ensure that the sandeels' role in the ecosystem is maintained to give foundations for larger and more stable catch outcome by letting the sandeel spread to the whole area (Greenstreet, 2006).

The standard method for surveying the fish stock abundance (Simmonds and MacLennan, 2005), does not apply to full extent for sandeel because of the weak backscatter. This is mainly due of their cylindrical shaped body size (Fig.2), and the lack of swimbladder (Hassel *et a*l., 2004). The biological cost for not having a swimbladder is that it has to continously swim to avoid sinking in the water column. A characteristic feature of sandeel is that they have a tube shaped jaw, which expands forward when opened. Sandeel is also toothless. In conjunction with the large gills, this creates a vacume in the bucal cavity that sucks in prey, enabling them to digest feed more efficiently (Macer, 1966; Hassel *et al*.,

2003). The lifespan of sandeel is usually around 6-7 years (Macer, 1966). Sandeel spawning takes place at the same site as it occupy during its lifecycle. The eggs are laid on the seabed where it attaches to grains of sand, it can also sometimes can be taken by ocean current and be found together with other plankton (Winslade, 1971). After hatching the larvae swims in the open water masses and feed on plankton until they reach a lenght of about 5 cm. Later, the larvae adopt an adult lifestyle and settles down in the sand. Sandeel are known to have a very high mortality rate, where a large fraction of the younger year class diminishes from natural mortality each year. It is conceivable that all locations with good substrate are occupied by sandeel, which implies that the recruitment larvae class meets competition for space when they are ready to settle on the bottom. Lack of suitable substrates seems to be one of the most limiting factors for the stock (Hassel, 2003).

Fig. 2. Lesser sandeel (*Ammodytes marinus*) (Photo copied from fishbase.org).

Swimming behaviour is dominant during daytime, where they usually form tall schools with limited areal extension. The schools are relatively stationary around their respectable habitats and distributed in patches around the seabed (Macer, 1966). Sandeel's feeding period is mainly from the early morning and throughout the day. They feed in open water of various plankton such as large diatoms, bristle worms and crustaceans, while they rest and avoid predators by burrowing into fine substrate bottoms during the dusk and staying there during the night (Winslade, 1974). Swimming activity is largely associated with feeding and is dependent on the availability of food, light intensity and temperature. It's typical to observe sandeel around sandy ocean bottoms, but they can also appear over hard substrate bottom. A long period over hard bottom is avoided due to high risk of mortality. (Freeman, 2004; Holland *et al*., 2005). Sandeel can bury themselves extremely rappid into fine substrates, while underground it is capable of moving both backwards and in other directions by turning its head. During the winter period sandeel stay buried in the sand in a state of hibernation (Macer, 1966). According to observations made from previous surveys sandeel

show a tendency to mix in with other schooling species such as herring (*Clupea harengus)* and mackerel (*Scomber scombrus*) during feeding in open waters (Pitcher *et al*., 1985).

Sandeel schooling behaviour is quite characteristic (Mackinson *et al.*, 2005) with its distinct rectangular and compact form, they can be easily recognised from an echogram display. The volume and areal size of sandeel schools can vary to some extent and schools have previously been classified in three different sizes by small, medium and large (from conversations onboard Johan Hjort 2011, large schools may also be referred to as "towers" by fishing skippers). According to Jensen *et al*. (2003), sandeel schools show a vertical avoidance reaction towards vessel fishing gear. Other studies (Gerlotto *et al.*, 1992; Soria *et al.*, 1996) regarding fish avoidance shows patterns of horizontal avoidance being most significant for schooling fish, while vertical avoidance seems to be most common with species located at scattering layers. Sandeel are described by Winslade (1974) and Macer (1966) as a rather stationary species, and experience from IMR surveys, where they have been able to position the vessel on top of a school for a significant time, indicate that there should be less concern with respect to vessel avoidance for this fish, compared to other schooling species, like herring.

1.2 Sandeel and hydroacoustics

At present, most large pelagic fish stocks around the world are being measured in abundance with acoustic surveys (Simmonds and MacLennan, 2005). The traditional acoustic survey method assumes that the distribution and migration pattern of the species is known, and the identification of species is based on the echo signatures recorded during the acoustic survey. The linear relationship between the integrated echo intensity and density of the fish in the water column would then be recorded on echograms, showing the density and structures of the relevant school (Simmonds and MacLennan, 2006). To estimate the abundance of the fish stock, it is required that the acoustical backscattering strenght of the target is known (referred to as target strength (TS)), and that the reflective properties of the target (referred to as backscattering cross section (σ)) and relevant biological information of the species can be measured. (Nakken and Olsen, 1977; Simmonds and MacLennan, 2005). At present, there is a lack of accurate target strength data on sandeels. The main reason for this is the difficulties to resolve single targets for a split beam measurement due to the school packing density (Ona, 2007).

Earlier TS experiments which where conducted by Armstrong and Edwards (1985) and Kubilius (2009), confirmed that sandeels had a weak and variable backscattering. The variability seems to be connected with the dynamic behaviour of the fish during schooling and feeding activity, where the tilt angle distribution may rapidly change over short time periods. These changes where probably due to the anguiform body shape and body tilt during swimming activity of the fish. According to Johnsen *et al.* (2009), sandeel can be acoustically identified based on the characteristics of the measured frequency response of schools from 18, 38, 120, and 200 kHz echo sounder systems. This finding may be important for acoustic surveys where it is hard to seperate sandeel due to the presence of other schooling fish such as herring and mackerel.

Fishermen have the past years used different types of fisheries sonar to locate and harvest sandeel schools. Some issues regarding the use of sonar for detecting sandeel schools, is the uncertainty related to detection probability and efficiency of the sampling volume compared to echo sounders. When conducting conventional abundance estimations on scientific surveys with echo sounders, the degree og coverage is limited to the acoustic beam sampling volume (V_0), related to the effective beam width at the depths on the sandeel grounds. V_0 indicates the propagated sound in space that is contributing to echoes at any instant, and it is a useful measure for comparing the target detection performance between different equipment (Simmonds and MacLennan, 2006). When conducting large scale fisheries surveys with echo sounder, the ratio between the sampled volume and total ocean volume of the bank is very small. With respect to school detection perfomance between sonar and echo sounder, the difference can be measured with relatively simple equations. The ratio between covered volume of sonar and echo sounder is expected to be significant, when dividing the sampled volume area (V_{area}) over total survey (A_{total}). Gerlotto *et al.* (1999) compared the sampling volume between a sidescaning sonar and echo sounder. He found that the sampling volume of a vertical echosunder with an 10° beam at a flat 55 m deep bottom along 1 nautical mile was 0.49×10^6 m^3. The volume sampled by the sonar in the same bathymetric conditions at 70 m range was 7.13×10^6 m^3. In this case the echo sounder sampled 6.9% of the volume sampled by sonar. Gerlottos experiment was however conducted with sidescaning sonar while this survey will use an omnidirectional system.

According to personal correspondance with Prof. Ona on may 5, 2011, a challenging topic when conducting a sandeel surveys, is the small dimensions of the schools relative to the observation volume of the vertical echo sounder. On a typical sandeel bed of 5 x 10 nmi, the fraction of sandeel schools hit by the echo sounder beam is small, since the effective sampling

width of the beam is only about 3 meters at the median depth of about 30 meters. Bottom depth in the investigated area fluctuates between 30 - 80 meters and the survey uncertainty from areal coverage alone is therefore large, particular on fields with very few schools. The size of the school itself may however influence the school detection probability. It is believed that echo sounder data may not be very suitable for an acoustic survey on sandeel, because the probability of missing a schools on transect in a standard survey design is large (Ona, 2010). In this case, the true distribution of schools on the field may not be correctly reflected in the echo sounder data.

1.2.1 Sampling with echo sounder

When using conventional echo sounders on low or medium stock densities during scientific surveys, high degree of effort (number of transects) is required to reduce the variance associated with the spatial distribution of the fish. An echo sounder sampling ratio is related to its equivalent beam angle (ψ), and under optimal conditions it can detect all targets that passes underneath the vessel. The echo sounder effective sampling width depends on the operating frequency, beam swath width and range to the seabed. Modern echo sounders transmit simultaneously several frequencies with similar beam width at 18, 38, 120 and 200 kHz (Simmonds and McLennan, 2006). In order to compare the sampling performance between an echo sounder and omnidirectional sonar, it's necesarry to compute the covered volume for a nautical distance for each of the acoustic instruments. The elementary equation for echo sounder sampling volume, when c = sound speed and τ = pulse lenght, is defined as

$$V_e = A\frac{c\tau}{2} \quad . \tag{1}$$

The covered area can be defined as

$$A = \Omega r^2 \quad , \tag{2}$$

where Ω is the solid angle of the beam and r is the range from the transducer to the seabed. The solid angle of the beam is estimated from the cosine of the acoustic axis (θ) , and is defined as

$$\Omega = 2\pi\,[1 - \cos(\theta rad)] \,, \quad [sr] \quad . \tag{3}$$

The recieved signal that the transducer emits is only sensitive towards an enveloped area inside of the beam. It may be vizualised as the solid angle at the apex of the conical beam. and is defined as the equivalent beam angle ψ. In effect ψ is used to measure the width of the volume insonified by the transducer (Simmonds and MacLennan, 2006). According to Foote (1991) the equivalent beam angle starts at a – 3dB down the beam point and measured in logarithmic scale (dB). The measured beam swath angle of the EK60 onboard Johan Hjort was 6.4°, with corresponding equivalent beam angle at

$$10log(\psi) = -20.6 \quad (4)$$

which is

$$\psi = 0.0085 \quad .$$

The school detection probability on wether the school is detected by the echo sounder also depends on the dimension of the school. If the diameter of the school is very small, much less than the width of the echo sounder beam, the effective detection width perpendicular of the transect is $\psi r^2 = A$. At low mean depth, say 10 m less than the bottom depht. The beam diameter can be estimated as

$$dr = \sqrt{\frac{A}{\psi}} \quad . \quad (5)$$

Since the school can be detected also in the borders of the beam at both sides of the echo sounders beamwidth. The estimated detectional swath width of the echo sounder can be defined as

$$de = 2dr + \overline{ds} \quad . \quad (6)$$

Where $\overline{ds}$ is the mean diameter of sandeel schools.

1.2.2 Sampling with sonar

Sonar acoustic systems follows the same principle as echo sounder, but instead of one single vertical transmission the SH90 use 480 transmitting channels to form a pulse that envelopes in all directions (Simrad, 2009). It can therefore cover a much larger area compared to conventional acoustic equipment. The cylindrical multi-element transducer has a spherical array of transmitting elements used to form 64 beams that covers 360 degrees in perpendicular direction of the vessel (Fig. 3). The omnidirectional beam transmits with a vertical swath width of 7 degrees, and the beam angle can be electronically tiltet from +10 to -60 degrees (Simrad, 2009). Alternative, the sonar can also form a 60 degrees vertical sliced beam that cuts trough the water column at any angle (Fig. 3). The sonar can subsequently switch between each transmitting setting.

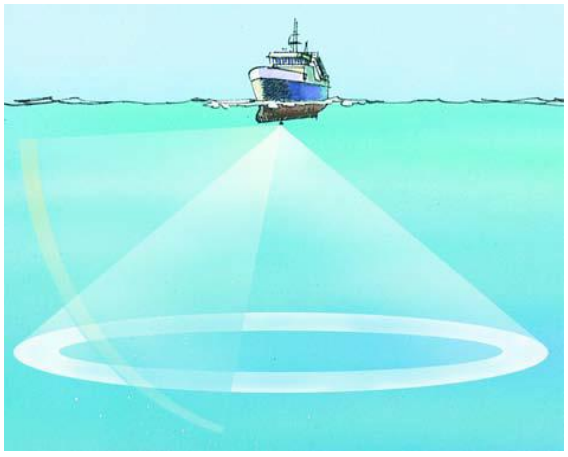

Fig. 3. Illustration showing the omni-sonar principle, with the vertical sliced transmisson on the vertical plane. (Image from Simrad.no)

The detection range is determined by its operating frequency (114 kHz) that enables more sensitivity towards smaller targets, but at the same time limit the range to around 300 meters (Simrad, 2009). The exact covered volume of a horizontal transmission is hard to estimate because the geometric shaped beam is curved by oceanic stratified regions (Misund *et al.*, 2000). The propagational sound speed is seldom linear due to the temperature and salinity variations trough different depths in the water. Thermal fluctuations are considered the most influental factor (Brehmer *et al.*, 2006). Misund *et al.* (2000) describes a simple model for estimating sonar sampling depth for a vertical transmission beam,

$$dm = tan\ \alpha\ (\frac{R1+R2}{2}) + D_1 \quad . \tag{7}$$

The equation estimate the middle depth of the vertical beamwidth α. R_1 and R_2 is the inner and outer detection range of the sonar for a school on a optimal horizontal plane and D_1 is the depth at transducer point. The inner detection range R_1, around 50 m, is deducted from the estimation due to vessel noise and propeller wake. Assuming that sandeel schools can only be detected when they are fully visible inside the border of the sonar, around 10 m, and at any point inside the transmitting range at both sides of the vessel. See Fig. 4. The estimated detectional swath width (do) of the omni sonar along a transect can be defined as

$$do = 2(R_2\text{-}R_1\text{-}10m) \quad . \tag{8}$$

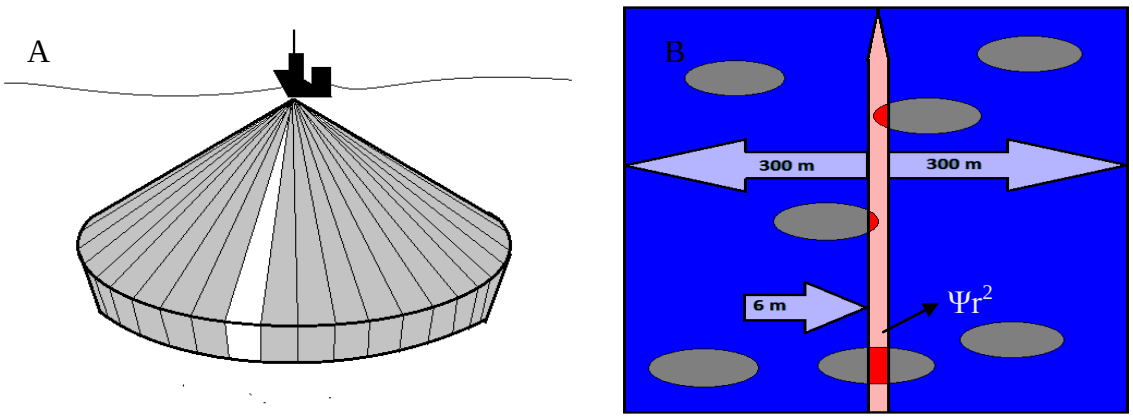

Figure 4. A) Representation of the omnidirectional multibeam sonar sampling volume around the vessel. The white beam represents the vessel heading. B) The relative detection swath width along a transect for sonar (blue) and echo sounder (pink). The diameter of the echo sounder swath with is estimated as $= 2dr + \overline{ds}$ and for the omni sonar = $2(R_2\text{-}R_1\text{-}10m)$. The grey circles illustrate schools along the transect. The red marking inside the echo sounder track illustrate the school area detected by the echo sounder.

1.3 Challenges with sonar

Earlier sonar models (mainly the SH80) have been tested on surveys before, but on other species than sandeel (Løkkeborg *et al.*, 2012). Due to the vertical beam width of the transducer, oceanographic conditions and relatively shallow bottom depth in combination with the weak backscattering from sandeel, the expected detection ranges were quite limited.

For this experiment the current model (SH90) has a new transceiver with improved data outputs and backscattering filter. The benefits is improved detection ability of targets with weaker target strenght (TS) and where schools are inherently distributed with respect to their neighbouring schools. It was also expected that new omnisonar data may be used to study the distribution of school patchiness in relation to the covered area, which is relevant for a potential adaptive choice from a survey standpoint.

Backscatter from sonar transmissions is also disturbed by noise and reverberation from bottom and ocean surface (Fig. 5). It is therefore important to apply an ideal tilt to the sonar beam. Under non-ideal conditions such as large waves and wind, the sonar beam may also be exposed to transmission loss due to sound attenuation that causes large blind zones at some distance from the vessel (Brehmer *et al*., 2006). The SH90 software is provided with various filtering options such as reverberation controlled gain (RCG), automatic gain control (AGC) and ping to ping filter to reduce unwanted echo interference and to receive a clearer sonar image.

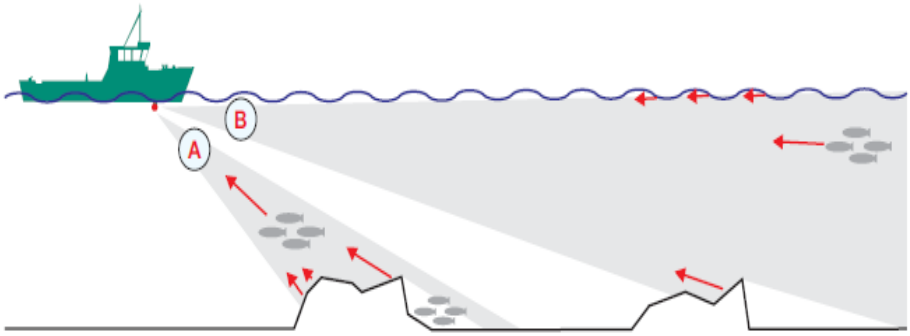

Figure 5. Example of sonar transmission reverberation. (A) Echoes from the rugged bottom terrain interfering with scattering from schools. (B) Interfering echoes from the ocean surface and bottom. (Image from Simrad.no)

When surveying, the target echo is dependent of the scattering properties of the target, school volume, density and the position of the school related to the transmitted beam. If a school is partially hit by the beam, size parameters and backscatter strenght will be incorrect. The correct measurement of the area is when the beam covers the entire school. For this survey we used an average tilt by - 6° wich would give an optimal range for initial detection between 50 - 250 meters range and around 25 meters depth, related to the transducer beam. (Fig. 6)

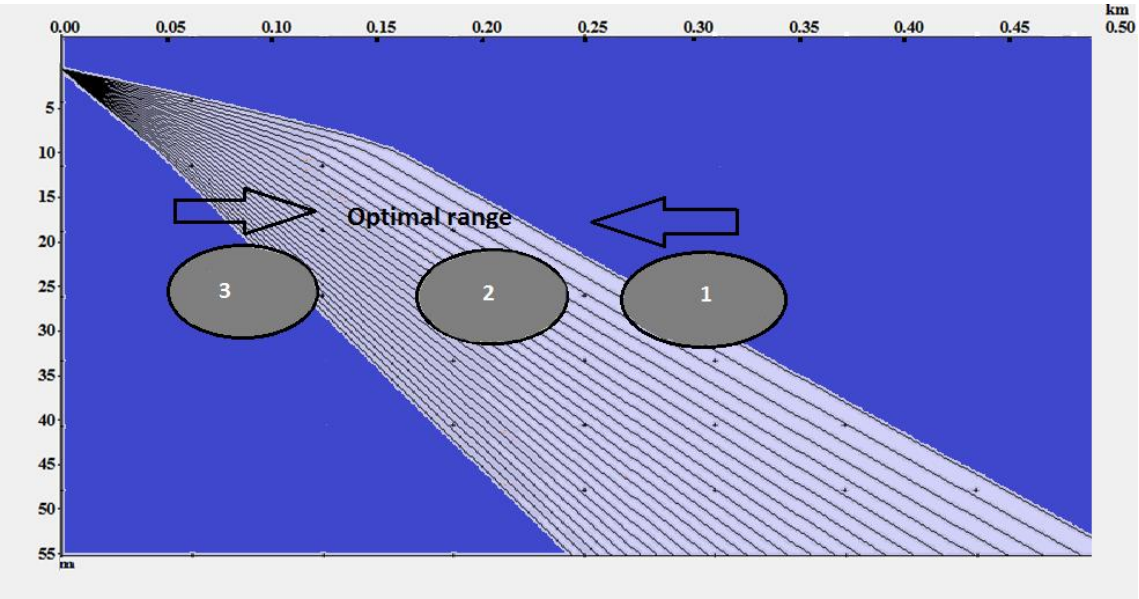

Figure 6. Image showing the optimal range and depht for a school to be hit by the sonar beam. The sampling resolution decreases with range (m). School 1: Low backscatter, high sampling resolution. School 2: High backscatter, medium sampling resolution. School 3: Medium backscatter, small sampling resolution.

According to Misund *et al*. (2000) recorded avoidance reaction from schooling fish towards approaching vessels creates a lateral avoidance reaction away from the vessel path at some point from the vessel. This should be considered when estimating the fish density because of the difference in distribution of schools recorded between a vertically directed echo sounder and horizontal guided sonar. Behavioural reactions related to the vessel are generally observed from fast swimming pelagic species such as herring and mackerel where the beam is most narrow and the vessel stimulus stronger (Pitcher *et al*., 1996; Soria *et al*., 1996). While sandeel is considered a fairly stationary species (Winslade, 1974; Macer 1966) with most activity between the water column and seabed, it is not expected to have the same degree of behavioural reaction compared to other schooling species (Greenstreet et al., 2006). Tracking of schools is relevant to observe any migration pattern present. According to Misund (1990) and Aglen (1994) interpretation of behaviour as a true migration or vessel avoidance reaction may be hard to distinguish. Aglen (1994) describes schooling fish may try to avoid vessel proximity which might influence backscatter due to fleeing reaction compared average schooling backscatter. Other studies (Gerlotto *et al.*, 1992 and Soria *et al.*, 1996) shows patterns of horizontal avoidance being more significant for schooling fish, while vertical avoidance seems to be most related with species located at scattering layers.

1.3.1 Data interpretation with sonar and echo sounder

Behaviour of school migration has been sucessfully recorded with sonars in past years (Halfsteinsson *et al*., 1995; Misund *et al*., 1995). Here the principle of data extraction and post-processing was to calculate the observed target coordinates relative to an orthogonal reference mark inside the sonar range. Fish school parameters were also calculated in relation to the vessel's speed and heading (Brehmer *et al*., 2006). The large sampling volume enabled tracking of a number of schools at a large distance from the vessel (1000 m under optimal conditions). For acoustic surveys with echo sounders there is already established a robust method for scrutinizing species and biomass estimation with post-processing software Large Scale Survey System (LSSS) (Korneliussen *et al*., 2006). However, the large amount of data collected during a sonar conducted survey, requires a special method for processing. Interpretation of SH90 raw files is still at development stage and this experiment would use post-processing software PROFOS (short for "Processing of fisheries omnidirectional sonar") as an additional build on the LSSS, as well as the image editing program ImageJ (Abramoff *et al*., 2004). PROFOS is designed to measure geographical coordinates, backscatter (dB) and schools parameters inside the sonar range where ImageJ is used to process large stack of screenhots from the actual sonar diplay.

1.4 Adaptive sampling and survey effort with sonar

Mapping total stock distribution abundance requires a selected range of data from a survey. A persistent challenge is estimating the size of a population from a limited sample. Statistical theory provides a number of design-based methods for estimating the mean density or total population size. These methods are primarely designed for independent sampled units where the underlying school distribution is fairly normal, such requirements are rarely met by actual fisheries data (Connors *et al.*, 2002). Most surveys are designed with a randomisation factor, sample allocation and area stratification to achieve some degree of consistency during an operation. Sampling design is carefully planned to minimize the variance from each survey, where accuracy and precision are the used terms to describe the deviations from the true value and consistency between samples (also referred to as bias). Main influence of variance derives from the survey sampling of a spatial distribution of the population. Such

school aggregations or “patchy” distribution results in very high variances when estimating the population because of strong skewness and local correlation (Connors *et al.*, 2002).

Indications based on sandeel stock data from previous surveys, (Ona, 2007) suggests that sandeel schools are patchy distributed with detection probabilities varying from low to high frequencies. According to Harbitz *et al.* (2009) this is considered a high-bias source when collecting data that impact the sampling result with high area precession and low sampling accuracy. Connors *et al.* (2002) estimated the sample variance of a stock size, when school densities in nearby sampling units were independent. Here, the ideal design-based approach was to use cluster-sampling formulas with the survey transects being the primary unit. Guillard *et al*. (1992) used a geostatistical approach to provide an confidence interval less than 20% of the estimated mean value of the average biomass. With prior knowledge of population distribution, the choice of a linear variogramme is a useful method for providing an estimate of spatial correlations between all samples. According to Petitgas *et al.* (2003), this is the most applied estimation model when conducting a hydroacoustic survey. This geostatistic approach may forecast the total stock size by predicting stock density in unsampled regions of the survey area. An adaptive cluster-sampling model (ACS) may be applied where the data are strongly correlated with target stock trends of concentration in dense clusters, rather than being evenly distributed over the survey area (Connors *et al*., 2002; Thomson, 1990). This type of school distribution is frequently observed from earlier sandeel fisheries data. ACS methods are typically applied with surveys where transects are the primary unit and the integrated sampling units are the secondary units. All the sampled units in the initial design should meet a pre-specified identity criterion determined by the researcher for the target species (Connors *et al*., 2002; Thomson, 1990). Sandeel schools are usually identified by their weak backscatter (TS), frequency response and schooling shape.

A common method for reducing uncertainty of biomass estimations is to apply stratification on the total search area. The splitting of fields to smaller areas is determined by prior knowledge of stock densities from earlier surveys. Stratification also requires knowledge about stock influencing gradients such as bottom topography, ocean depth and seasonal temperature and salinity (Simmonds and MacLennan, 2005). Assuming that sandeel are cluster distributed, an adaptive survey is the preferable survey method. The two-stage adaptive survey (Fig. 7) is designed to systematically improve the precision of results by reducing or removing effort where there is no fish (Simmonds and MacLennan, 2005). The first stage is concentrated on collecting data from all strata (total survey area). When comparing all strata, the second stage of the survey would take place on the stratum that has

the largest density of schools. The sampling intensity over this particular area should then significantly increase with more frequent transect lines (Harbitz, 2009).

According to Aglen (1983) the degree of coverage (DC) is the used term to decribe the sampling intensity from sailed distance (N) is relative to the square root of the investigated area (A),

$$DC = N/\sqrt{A} \quad . \tag{9}$$

DC is a unit of effort and which influence the precision of the surveyed area independent of size e.g. the standard error of abundance estimates decreasing when DC increase. Aglen (1989) describes another measure of effort estimated from repeated surveys, the empirical relationship beetween coefficient of variation (CV) and DC. The CV relationship does not give a good estimate from a single survey, but is a useful guide of the amount effort needed to obtain a wanted precision (Simmonds *et al*., 1991). The relationship can be described as

$$CV = 0.5/\sqrt{DC} \quad . \tag{10}$$

If we want to sample an area of x nmi^2 with a desirable CV in %, DC needs to be at least

$$DC = (0.5/CV)^2 \quad . \tag{11}$$

The required survey lenght in mni can then be calculated from

$$N = DC \cdot \sqrt{A} \quad . \tag{12}$$

Additional use of sonar together with echo sounder is believed to significantly decrease DC/CV relationship and reduce the search effort. The detectional swath width of sonar (do) or echo sounder (de) may therfore be included in DC estimation (N (do/de)) to demonstrate the potential difference on the survey effort. The improved search range of sonar is believed to give a better overview before undertaking an adaptive choice.

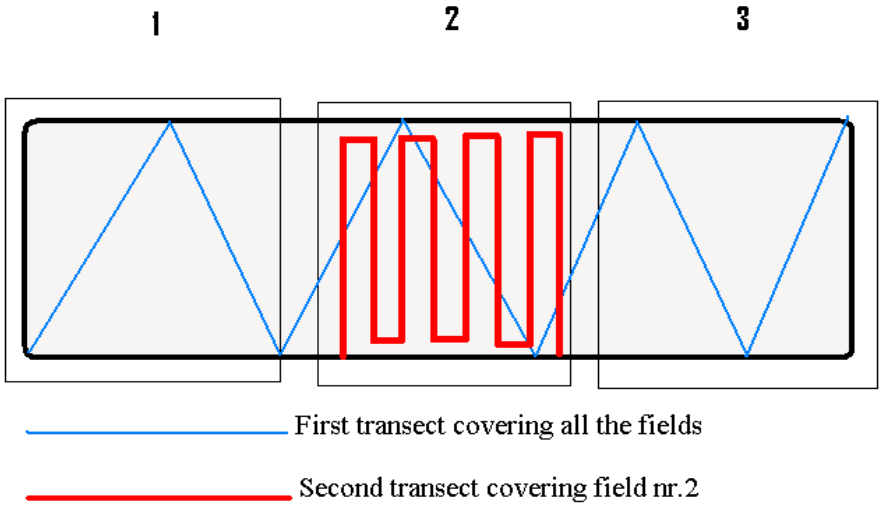

Fig 7: Illustration of the two-stage adaptive survey principle. The total survey area (black) is divided into three smaller strata by numbers. The blue line represent the first stage of the survey by transects over all the strata. The red line represent the second stage of the survey, with more frequent transects over the stratum with the largest school density measured from the first stage.

2. MATERIALS AND METHOD

2.1 The study area

The sandeel survey was conducted in the North Sea approximately 90 nmi of the Norwegian coast during the period April 26 to May 08, 2011, by the research vessel Johan Hjort (64.5 m, 1950 tons, 3264 hp). The primary objective of the survey was to collect data with the EK60 echo sounder and to measure sandeel abundance that could be used as an advice for the sandeel fishing quota in the Norwegian sector of the North Sea. For this particular survey Johan Hjort had acquired the newest fisheries sonar model (Simrad SH90), which was used during the entire survey for detecting sandeel schools as a secondary objective. The survey was planned to cover most of the sandeel grounds of the Norwegian sector of the North Sea by sailing fixed transects over each of the main sandeel grounds. On each ground, the survey was accomplished by a randomly selected starting ground point and by a number of transects, covering the ground with a fixed degree of coverage (Fig. 8). Included in this thesis is the data from two of the grounds, the "Inner Shoal East" and "Hardangervidda". During the survey 8 standard CTD casts were taken from Hardangervidda, together with 5 biological samples from a towed modified scallop dredge (DuPaul *et al*., 2003; Mackinson *et al*., 2005) and the Campelen 1800 bottom trawl (Engås *et al.*, 1987). The survey on Inner Shoal East had 5 CTD casts and 7 biological samples. Trawling was conducted on acoustically indentified sandeel schools and restricted to daytime only. The scallop dredge was used by day and night to sample fish burrowed into the seabed. Biological sampling was systematically located in areas with a high acoustic sandeel density. All catches were sorted by species, weighed and measured in lenght according to Mjanger *et al*. (2000). For large catches, the lenght of 100 sandeels was measured in a randon subsample.

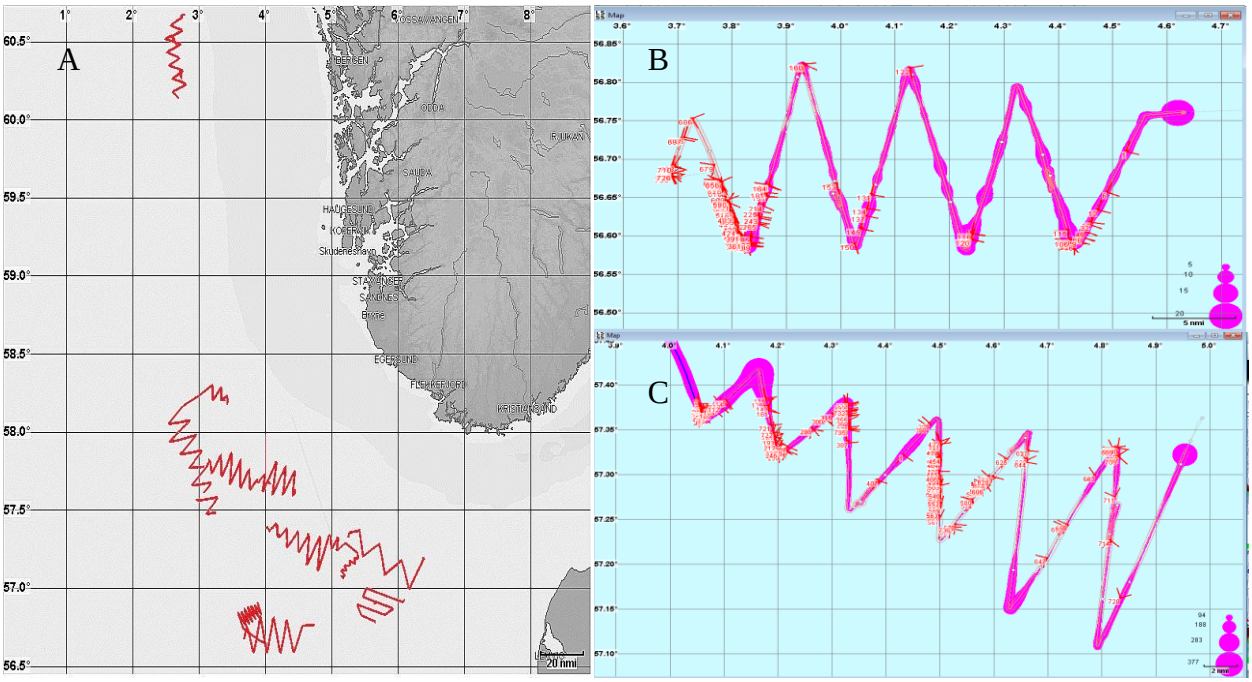

Figure 8:A) Map of the Norwegian coast displaying the position and transect of all the survey grounds on the sandeel survey. B) Map showing the two sandeel banks crutinized with LSSS and PROFOS, Inner Shoal East (B) and Hardangervidda (C).

2.2 The fisheries omidirectional sonar (Simrad SH90)

The multibeam omnidirectional fisheries sonar used for this survey was the latest Simrad model SH90 (Fig. 9). With a 114 kHz operational frequency and improved filtering ability, it was expected that the equipment would be able to be detect sandeel schools. The sonar was mounted on the ship's hull unit so the transducer head could be lowered about 1 meter beneath the ship's keel. The electronic control unit for stabilisation of the sonar beam was also mounted on the hull unit. When the stabilising system is active, the tilt angle is automatically corrected relative to the vessel's pitch and roll movement induced to the vessel from ocean waves. The transducer head is configured with 480 individual transmitters distributed on sixteen transceiver circuit boards, each transmitter is individually addressed and controlled from the signal processor (Simrad, 2009). Controlled settings included power output and time delay for each transducer element in order to form the requested beam with desirable tilt angle, also called beamforming (Simmonds and MacLennan, 2005; Bremer *et al.*, 2006). The outgoing transmission is capable of covering a 360° perpendicular area of the ship with an option to stepwise tilt the beam angle at +10° to -60°. Detailed overview of sonar

specifications can be viewed in Table 1. The most common tilt angle used during the experiment varied between – 4° to -7° depending on bottom and the position of the target species in the water column.

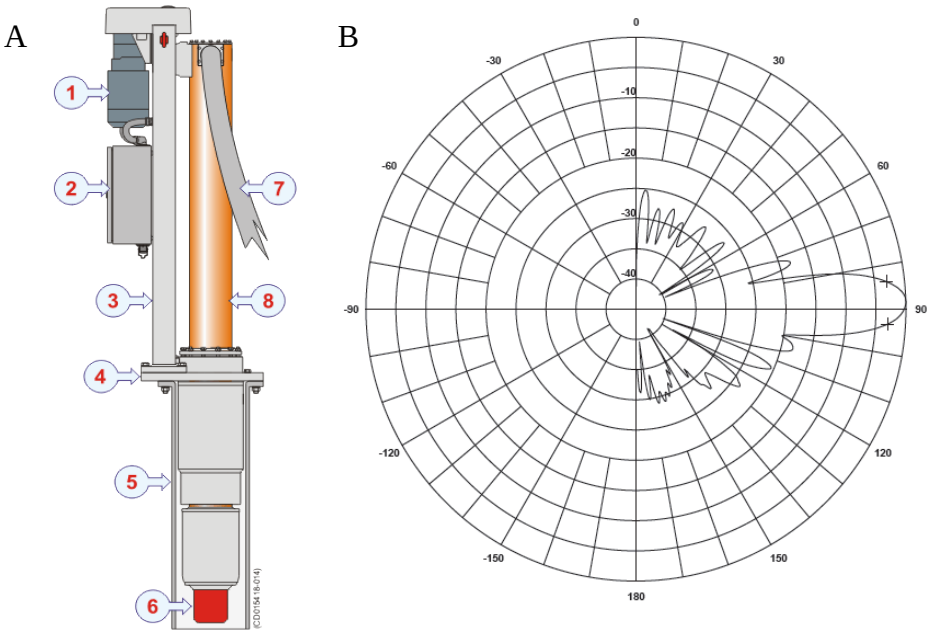

Figure 9: A) The SH90 body and transducer. 1: Hoisting motor. 2: Motor control unit. 3: Hoisting unit. 4: Mounting flange. 5: Installation trunk. 6: Transducer. 7: Transducer cable. 8: Transducer shaft. (Image from Simrad.no) B) Picture of the transmitting beam pattern from omnidirectional sonar . Beam width α is 7°. (Image from Brehmer *et al.*, 2006)

The SH90 sonar transmits with a frequency modulated (FM) pulse centered at 114 kHz with a half power beam width of 7°. The pulse duration τ for each ping was 26 ms at 5 kHz bandwidth. The time varied gain (TVG*)* applied during the recording was 20 log R + 2αr, but the raw data is recorded without TVG. Table 2 shows the specific configuration setup and sonar settings for this experiment. The sonar detection range for strong schools at this frequency are potentially 1000 meter under optimal conditions, while the effective range depends on school target strenght, environmental parameters affecting sound propagation and bottom/surface reverberation. The sonar operating frequency is usually the first limitation for school detection range due to increasing absorption coefficient with frequency. (Simmonds and MacLennan, 2005) The sonar's transmitted sound intensity profile is measured or computed from CTD measurements. We have used Lybin (Hjelmervik *et al.*, 2008) to simulate the sound propagation in the sandeel survey area (Fig. 10). Lybin is an acoustics ray-tracing model that gives an overview of the sound propagation conditions, given a known

sound velocity profile of the water column. The model is two-dimensional, covering depth and range. It estimates the transmission loss, the reverberation level and the noise level based on sonar parameters and environmental data such as salinity, conductivity and temperature. Data from several CTD casts have been entered to Lybin, and the sonar specifications loaded. These data are applied to the sonar equations for estimation of signal propagation. Detection theory is then used to find the probability of school detection and the corresponding detection range (Hjemervik *et al.*, 2008).

For this survey, detection range measured with Lybin where set according to bottom depth between 60 – 80 meter and bottom reverberation level at 6-9. This would limit the sonar transmission range to around 300 meters in omnidirectional width. All receieved signals beyond this point would be identified as reverberation noise from ocean bottom and ignored from the post-processing work afterwards. Foote *et al.* (2005) established a robust protocol to achieve a proper calibration for some multibeam sonars, however SH90 sonar was not calibrated at this point, as no calibration protocol for omnidirectional fisheries sonar is yet avaliable. Normal calibration procedure for the EK60 where conducted according Foote *et al.* (1987) just prior to the survey.

Table 1: The SH90 general sonar specifications

Simrad SH90 Multibeam Omnidirectional Sonar fact sheet:	
Sonar frequency	114000 Hz (114 kHz)
Transducer depth below ships keel:	1m
Tilt angle, Sender:	-6.0°
Tilt angle, Receiver:	8.0°
Beam Width, Sen:	5.5 °
Beam Width, Rec:	8.0°
Performance specifications	
Operational frequency**:**	114 kHz
Operational range:	Range steps: 50 to 2000 meters in 10 steps
Tilt and tip functionality:	Tilt: +10 to -60° in 1° steps
	Tip: +10 to -90°
Transmitter:	
Number of transmitter channels	480
Transmission modes:	360° omnidirectional
	180° vertical
Pulse modes:	CW (Continuous wave)
	FM (“Chirp” FM)
Number of individual elements	480
Beams:	
Horizontal transmission: 360 degrees	360 degrees
Horizontal reception:	8 degrees
Vertical transmission:	7,5 degrees
Vertical reception:	7,5 degrees
Vertical resolution (transmission + reception)	5,5 degrees
Beamwidth:	Narrow, Normal or Wide

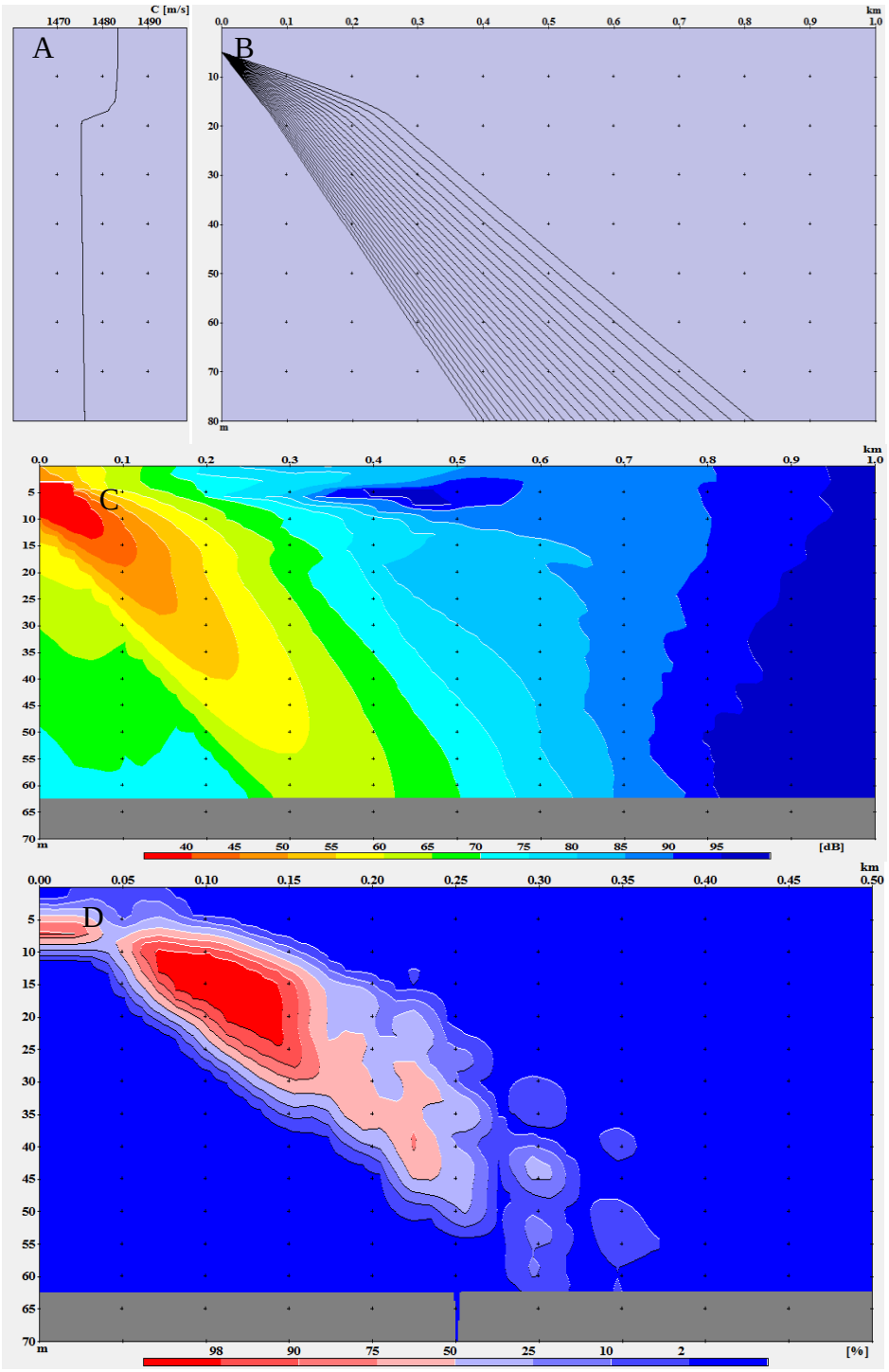

Figure 10: The sonar beam simulation software Lybin applied for the SH90. A) Show the sound speed, computed from a representative CTD profile taken from the Hardangervidda. The CTD profile is loaded into the program to give an accurate simulation of the sound propogation, given the depht of the transducer frequency, beam opening angle and the beam tilt. B) Show a cross section trough the acoustic beam with ray tracing. C) Shows an relative sound intensity plot (dB), which may be used to interpret the school detection probability. D) Shows the computed detection probability in % for one ping. We can conclude that the best range for the sonar at this depht and with the prevailing sound propagation is about 300 m. After this range bottom echoes may disturb the detection of schools in the water column at bottom depht 60 – 70 m.

2.2.1 The sonar processing of acoustic signal

The sonar image that is viewed on the computer screen is processed data with many different filtering options before displayed to the user. After the transceiver units in the transducer have received the echo signal, the initial echo response is exposed to unwanted noise. The image are therefore processed and interpreted by the computer in order to achieve a clear and stable presentation on the sonar display (Simrad, 2009). The first filtering device is the frequency modulation (FM), which is a sweep frequency where the receiver filters out the signals that are correlated with the ones that are transmitted. This efficiently reduces interference, noise and reverberation as well as it increases the sonar's detection range. The advantage with the FM correlation filter is that it retains a higher resolution in range with long pulse duration and it is less sensitive towards moving targets such as schools then other filters. Another filtering option is the automatic gain control (AGC) and reverberation controlled gain (RCG). AGC sense the echo level in several directions and use this as a basis to adjust all the transceiver beams. This will achieve an automatic scaling of the data in order to maintain proper range with respect to amplitude of the echoes. The RCG function adjusts the echo level in order minimize echo from surface and bottom reverberation. This is useful in shallow water where the RCG will effectively reduce the bottom and only display distinct but isolated targets. RCG setting is however sensitive to weaker and scattered targets e.g. schools that are close to the bottom, may be perceived as reverberation.

The processor unit is also able to compare the echoes from a selected number of transmissions (ping-to-ping filter). This setting can be used to provide a cleaner presentation by reducing the interference and noise by setting the assumption that an echo has to be present in a selected number of pings before it is presented. The ping-to-ping filter is also designed to remove unwanted noise from the sonar display by reducing interference from other acoustic systems (in our case the echo sounder), propellers and noise from other vessels. As with the EK60, the time variable gain function (TVG) is integrated in the sonar display. This function controls the gain of the receivers so that the schools are given a correct echo strenght (and colour) on the display inside the regulated TVG range. During our experiment the TVG was set to *2*0 LOG R. All of the relevant sonar display settings used during the survey can be viewed in Table 2.

Table 2: Relevant sonar setting specificatiosns used on the the survey

Sonar model	**SH90**
Tilt Angle (deg), transmitter	0° to -3°
Beam Width (deg), transmitter	Normal (7.5°)
Beam Width (deg), reciever	8°
Sonar display range (m)	300-600
Sonar frequency (kHz)	114
Pulse Mode	FM (26 ms, 5 kHz bandwidth)
Gain	20
Source level (dB)	211
TX Power setting	Low
TVG	20 LOG R
ACG, RCG, NF, PPF settings	Medium
Pulse lenght	0.9 - 75 ms

2.2.2. The sonar sampling procedure

The sonar data were recorded continuously during normal acoustic surveying and fishing operations, which are referred to as sampling scheme called prospecting mode (Brehmer *et al*., 2006). In prospecting mode all fish schools are detected along a predefined transect derived from a standard survey design. The intention of the survey was to record as many sandeel schools as possible with the sonar- and echo sounder systems, and compare the detection performance between each sampling volume. The sonar sampling mode was set to subsequently switch between the horizontal- and vertical guided tranmission setting. This sampling effect was also transferred to the raw files when later displayed in pre-processing mode. The survey was set up with matching clock syncronizations for each acoustic system (sonar and echo sounder) to record at the same time, this would enable *in situ* comparison during the experiment. Each survey transect started during the dawn in correspondance with sandeel diurnal migration (Jensen *et al.*, 2003). The survey continued throughout most of the day when there was daylight. During nighttime the vessel remained either stationary at the last stop position, or continued sailing a transport leg to the next survey area according to plans.

During the survey all the output data files was recorded from the echo sounder and sonar and stored for post-processing. The extracted sonar data files would fill up the hard drive space much faster compared to the EK60. The sonar was therefore set up to record data only during transects over sandeel areas in order to avoid using all hard drive space. During each transect we also manually recorded every potentially sandeel observations on the sonar and echo sounder. The number of schools for each sandeel area where maually counted by

capturing screenshots from the sonar display (Fig. 11), while the data for post-processing was transferred with a ethernet connection from the main SH90 hub to the computer driving the display. The data was automatically stored on a external drive by a sonar recording software pre-installed on the sonar computer.

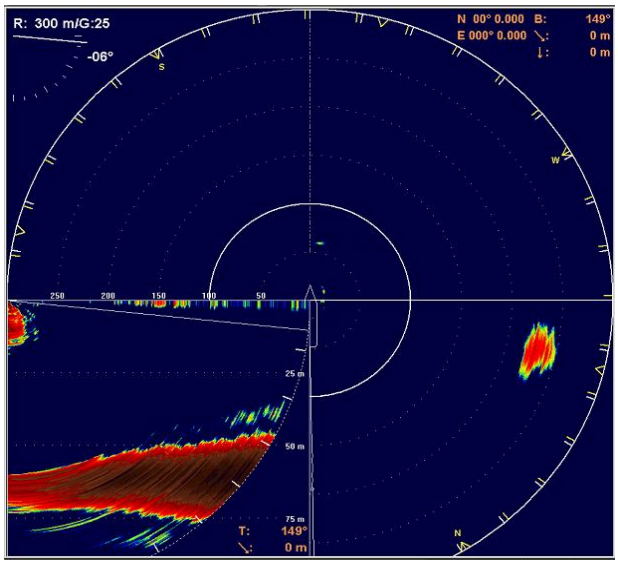

Figure 11. Example screenshot from the sonar display during surveying. A sandeel school is displayed on the bottom right area with strong red colour. The vertical reception is displayed on the bottom left window. Each ping interchanged between vertical and horizontal transmission.

2.3 Acoustic data analysis

The collected data was processed with two different methods. The data which where acquired from the screenshots of the sonar display was analyzed with the photo editing software ImageJ (Abramoff *et al.*, 2004), while echo sounder and sonar output files where analysed with LSSS and PROFOS respectively. The main objective for applying the ImageJ editing software to the sonar screenshots, was to estimate the size of the cross sectional area of sandeel schools, not avaliable to the echo sounder. The initial sonar screenshot displays schools in a perpendicular direction of the vessel, while the centre of the screen is the relative origo where the transducer is located (Fig. 12). An issue with respect to the school selection was to know exactly at what range the school area should be measured at. When recording a school in real time, the school area will frequently change or vary between successive pings and vessel range. An example is a sandeel school that changes its areal size from 1000 m^2 at 250 m range to 2000 m^2 at 150-meter range. In this case, the selected schools that were

processed with ImageJ were measured at the maximum point of areal size and backscattering strengt as measured from its colour (Sv). The intention behind this is to relate the optimal range for the sonar with the density centre of the school. In theory, the transmitted beam will cover the largest part of the school target when the received echo shows maximum Sv value and the areal size is at maximum (Fig. 6). This issue however, requires some knowledge about sandeel school dynamics. In total, 750 schools were scrutinized with a high probability of being a sandeel from all the total screenshots stored.

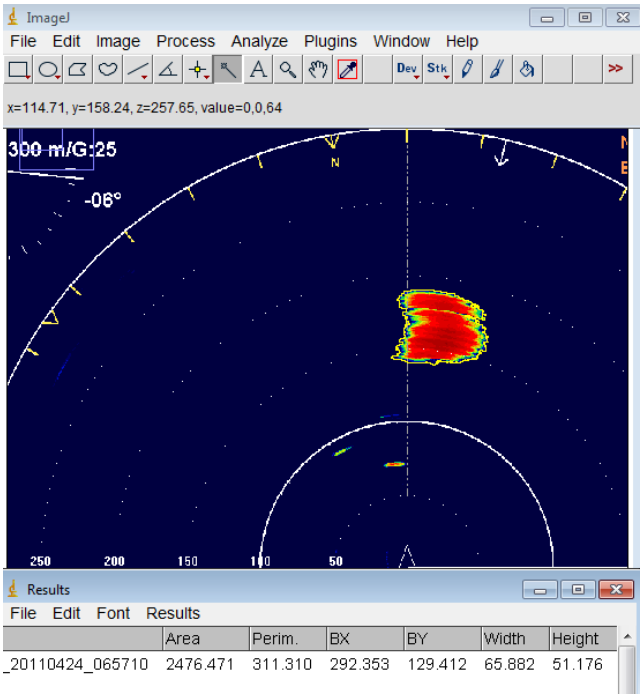

Figure 12. Example image from ImageJ used to detect and process screenshots from sonar the display and to measure the shape and area of sandeel schools. (Screenshot from sonar display viewed in ImageJ)

2.3.1 Calibration of the sonar display in ImageJ

The initial sonar display has a overlaying range scale, with clear range indicators and angular orientation marks in the horizontal direction (Fig. 12). This diplay also include sonar settings, navigation parameters with vessel and target positions. According to Simrad (2009), the scale indicator is true range and direction as long as the sound speed is entered correctly and the sonar head misalignment is accounted for. If the scale is digitized with the sonar image, true measurements may be made on the image. When importing the screenshot stack

of sonar images to ImageJ, the intial scale and distance are measured in number of resolution pixels (p) per. picture (1280 · 1024), which can be expressed as

$$\textit{Digitized area, whole area frame} = DX \cdot DY = 1280\ p \cdot 1024\ p \quad , \tag{13a}$$

$$\textit{Digitized area, sonar area display} = X1 \cdot Y_1 = 1020\ p \cdot 1020\ p \quad , \tag{13b}$$

$$\textit{True scale sonar display area} = X2 \cdot Y_2 = 600\ m \cdot 600\ m \quad , \tag{13c}$$

$$1020\ p = 1020\ p = X1 = Y_2 \quad , \tag{14a}$$

and

$$600\ m = 600\ m = X2 = Y_2 \quad . \tag{14b}$$

The prelimanary assumption for calibrating the true scale of the sonar image is

$$X_1/X_2 = Y_1/Y_2 = 1020\ p/600\ m \quad . \tag{15}$$

When the known distance of the sonar's detection limit is 300 meter at any range then

$$X_2/2 = Y_2/2 = 300\ m \quad . \tag{16}$$

The global calibration factor for the true range of the sonar display is

$$\frac{X_1/X_2}{2} = \frac{Y1/Y_2}{2} = 510\ p/300\ m = 1.70\ p/m \quad . \tag{17}$$

This means that 1.7 digitized pixel in the screenshot equals l meter in true range. In ImageJ it is possible to manually measure any given lenght in pixels and change that to whatever desirable scale as global setting for all images.

2.3.2 Measuring school area, perimeter and range according to vessel

A useful application in ImageJ was the "wand" tool, which enabled an automatic detection drawing of the border of objects with colour gradients as the distinct seperator. All of the sonar screenshots is displayed in RGB format, referring to the colours red, green and blue. Colour in the image, is compiled from three different hues of colour mixed together to

form any of the other colour. When the highest intensity of each colour is mixed together, white light is formed, while at zero light intensity the image is black. The recorded schools from the diplay screenshots features a RGB compilation with blue as dominant gradient with red at highest intensity for schools. Fig. 13 shows a typical RGB profile from a school where the entire school is marked. The wand tool was used to automatically draw a detailed outline of the targeted area down to pixellated level. The selection criterion locates the nearest threshold of the RGB gradient from the school boundary and marks a perimeter around the target (Rasband *et al.*, 2011). The default automatic thresholding function used by the wand tool, to separate the image into objects and background. It does this by computing the average of the pixels at or below the threshold. The wand tool stops where the threshold is larger than the composite average (Rasband *et al.*, 2011),

$$Threshold > (Average\ background + Average\ objects)/2 \quad . \tag{18}$$

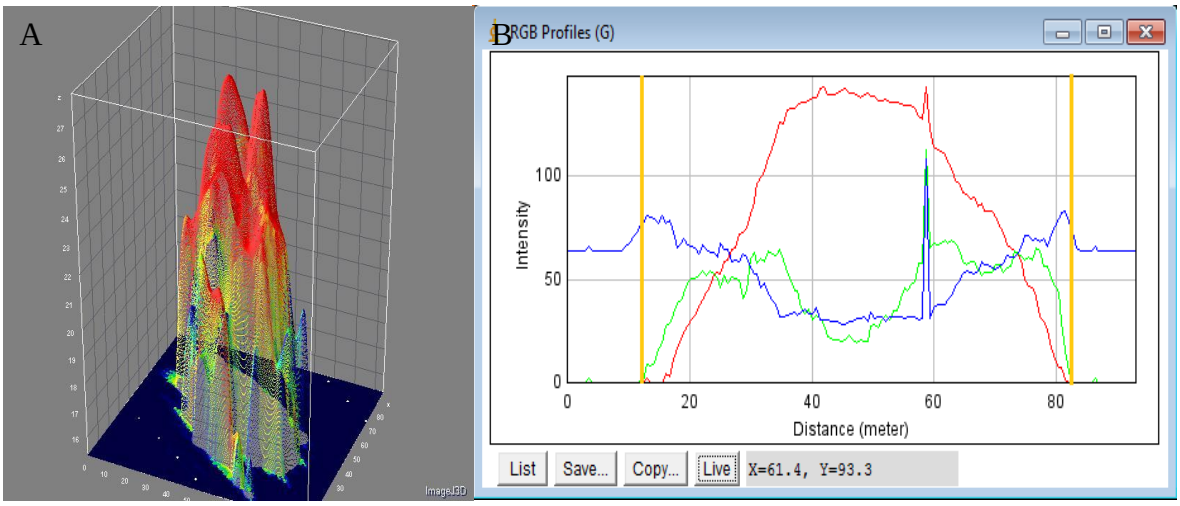

Figure 13: A) ImageJ showing a sandeel school in 3D at pixellated level from the sonar screenshot. The wand tool is used to mark a perimeter around the school. ImageJ converts the marking to 3D by using colour intensity as z value. B) The RGB profile of a typical sandeel school. The green and red curve is the area where the border of the school starts, while the blue colours display the background (surrounding water). Two yellow markings are added to show the external boundary of the school.

Based on the desirable selection, area, lengths and orientation angles to point coordinates was calculated and displayed in a seperate result window. The area of the object was calculated by adding up all the pixels inside the selected line by brightness value. When the known calibration factor of 1.7 pixels are equal to one meter, the added sum of square

pixels inside the area of selection would be adjustet to match the scaled value. With line selection the following parameter would display the range and angle of the school in relation to the vessel. The line was manually selected from the origo (vessel point) of the sonar display and stretched to the middle of the school. The recorded lenght and angle from the straight line was calculated by the number of pixels along the selected line and divided by the calibration factor. The object perimeter is the same as the lenght of the marked school boundary and calculated in same manner as the length (Fig. 14). The school diameter was estimated from the areal value,

$$D_s = 2\sqrt{\frac{A}{\pi}} \quad , \tag{19}$$

when assuming that the schooling shape is approximately circular.

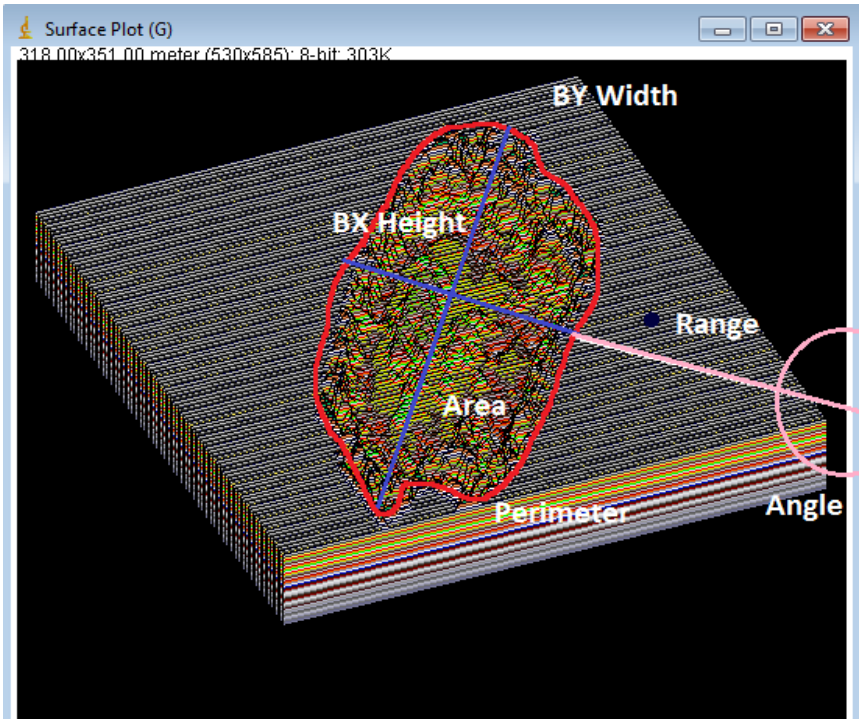

Figure 14. Surface plot of a sandeel school viewed in pixel format in ImageJ. The following parameters are displayed in the figure: Range (m), Angle (degrees), Perimeter (m), Area (m^2), BX Height (m) and BY Width (m).

It was necessary to correct the school parameters due to the sonar beam width. Each school was observed within a horizontal range, which allows a novel extrapolation of true school area according to Misund *et al.* (1995). The true value of area (A) decrease as the

vessel approaches the school. Our data set did not include multiple range and areal measurements of the same school, but it was possible to correct the true school width (BX) along the beam and height (BY) across the beam with the following equations

$$Lw_{corr} = BX \cdot \cos(T) - (c\tau/2) \quad (20)$$

and

$$Cw_{corr} = BY - 2R \cdot \tan(\alpha/2) \quad . \quad (21)$$

Where cos(T) is the cosine of the tilted angle of the sonar transmission (-6°) subtracted with sound speed (c) estimated from CTD casts and pulse lenght(τ) according to sonar range (300 m). R is the range of the school from vessel and tan (α) is the tangent of the beam width (7°).

2.3.3 Analyzing with PROFOS

LSSS and PROFOS were used to process the output files from EK60 and SH90 respectively. Detailed description of the LSSS proccedure for the echo sounder and Korona pre-processing setup is referred to in Korneliussen *et al*. (2006). Current PROFOS version used for this experiment worked as a prebuild add-on to LSSS, and mainly used to observe and scrutinize fish schools from surveys conducted with omnidirectional fisheries sonar. The program is under development and therefore to some extent unstable when processing large files. PROFOS was initially developed for the former sonar system used on IMR vessels the Simrad SH80. After the SH90 was introduced, PROFOS needed to be customized in order to read its new output file format. This lead to the consequence that the applied transducer settings used for interpretation of sonar range and tilt parameters was regarded as erroneous by the processing software. Because of this, scrutinizing the sonar data was extremely time consuming, and it was decided that only two areas of the total sandeel survey should be scrutinized and compared in this thesis; Hardangervidda and Inner Shoal East (Fig. 8). The initial assumption was that the echo sounder results from Hardangervidda had a high density of clustered sandeel schools, while Inner Shoal East did not. They were therefore representatives for two extreme situations.

Scrutnizing with PROFOS is similar to ImageJ in the sense of visual representation. Instead of using screenshots from the sonar display, the acustical raw data are visualised on the echogram as a display of echo strengths (dB) from each ping. It was possible to run,

rewind and fast forward the collected survey data from successive pings with corresponding volume backscattering strenght (Sv, dB) displayed in the colour bar (Fig. 15). A school was defined by a mask on the acoustical samples of one or more pings and could be grown as a school in the interpretation, by selecting a seed on the SH90 display. The growing algorithm works by starting the selected seed point and then advancing to neighbouring samples that satisfied the predetermined school criteria. PROFOS was designed to not allow grown schools to overlap in the same ping and geographically on neighbouring pings. For a school sample to be grown, the criterion had to be compatible with the following sample tresholds.

Minimum value: The voulme backscattering strenght, Sv (dB) of a sample had to be greater or equal to a -45 dB threshold
Max value: The voulme backscattering strenght, Sv (dB) of a sample had to exceed a level of -20 dB
Max ping from seed: School had to be present on minimum 10 pings, before or after the distance from the ping containing the seed point.

School samples had to be positioned outside a designated blind zone and inside the sampling range of the vessel, which was configured in the transducer setting. The blind zone for this experiment was set at 50 m around the vessel to eliminate the sonar transmit pulse and vessel reflection from the sonar interpretation. Additionally a blind sector of 25 degrees where set to cover the stern part of the vessel in order to remove potential echoes created from the propeller water (wake) of the vessel. The effective sampling range were set at 300 meters, and any echo signal beyond this range were be neglected from the scrutinizing process. After a school was grown, it could be manually edited in the *edit-working mode.* If necessary, a selected school could be deleted, increased or decreased in size to a desirable state, and merged into one with another school or extended to include neighbouring pings. School, sonar and ship parameters calculated by PROFOS are displayed in Table 3.

Table 3: School, ship and vessel parameters calculated from PROFOS

PROFOS parameters	
Time per school:	*StartDate:* With format yyyy-mm-ss. *StartTime:* With format hh:mm:ss.xx where xx denotes hundredths of a second. *StopDate:* With same format as StartDate. *StopTime:* With same format as StartTime.
Geographical bounding box per school:	*Box.lon.min:* Minimum longitude. *Box.lat.min:* Minimum latitude. *Box.lon.max:* Maximum longitude. *Box.lat.max:* Maximum latitude.
Depth	The depth per school is defined as mean value of center depths per ping
The area per school:	*Area.mean*: Mean value of area per ping. Area is calculated from school masking grid and relative range. The area is not corrected for beam width or sample length
The ping count per school:	*Pings:* Number of pings where school is defined. Pings between school start and stop where the school is not defined (empty school mask) are not counted.
The motion per school:	*Speed:* Speed in m/s. *Heading:* Heading in degress. Both speed and heading are calculated using the first and and last center points. If the school is defined on only one ping, these values are marked as N/A.
The school center per ping:	*Center.lon:* Longitude of the center. *Center.lat:* Latitude of the center. *Center.dep:* Depth of the center. The center point is calculated purely geometrically and does not represent the mass center of the school. The center depth is calculated assuming perfectly straight beams.
The mean value per ping:	*Sv.mean:* Area weighted mean value of all samples in the school. The mean value is in dB, but the computation is done with linear values.
Ship info:	*Ship.lon:* The longitude ship gps position. *Ship.lat:* The latitude ship gps position. *Ship.speed:* The speed along ship. *Ship.heading:* The ship heading. *Trans.tilt:* The transducer tilt.

After a school was grown, a unique ID was assigned to the position and relative swimming directions were displayed as vectors over the survey map (Fig. 16). PROFOS is also able to split and merge single or multiple schools with allocated identity tags, which is useful when observing aggregative schools at mesoscale and limit the effect large schools can have on smaller neighbouring schools. (Petitgas *et al*., 2001)

PROFOS worked together with LSSS to provide a transparent display between EK60 and SH90 data. However, the tranducer settings in PROFOS were not compatible with the current sonar model output file format. This caused a miscalculation of the school parameters and transducer setting for tilt (°), depth (m) and school speed (m/s). This information was therefore discarded from the analyzing result.

Personal criterias for selecting and growing schools with PROFOS were based on various assumptions and experience. The assumptions made for a sandeel school to be selected, were the following; School usually appear at 150-300 m distance from the vessel, target species should appear on at least 3 or more successive pings to ensure that the echo does not originate from noise. Scattering volume (Sv) should not be less than -44 or stronger than -32 dB. Most of the detected schools had a mean Sv between -42 and -37 dB. In most cases where detection of herring schools occurred, the mean Sv was notably higher, around -35 dB. It was expected that a swimbladdered species such as herring could generate significant stronger backscatter compared to sandeel (Redwood, 2004). Unknown schools with high backscatter would therefore be categorized as herring in the scrutinizing process.

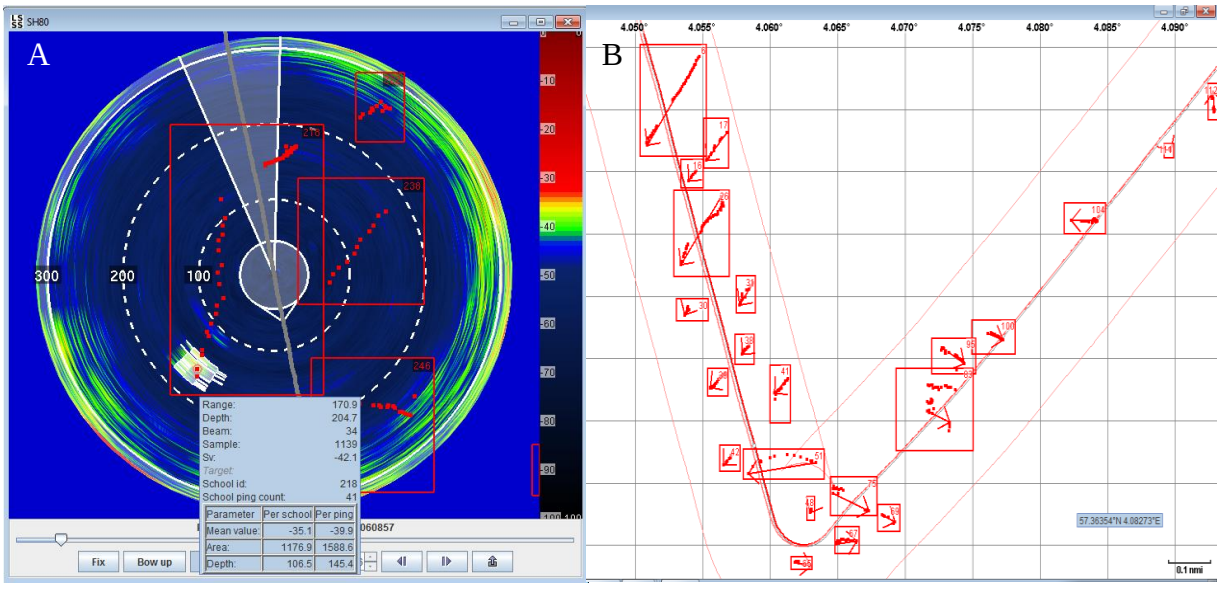

Figure 15. A) Working display of the PROFOS post-processing software. The image is generated from the sonar's scientific output files and display all the echoes created in one ping. The highlighted area (white colour)

is a grown school. The red frames inside the sonar display shows recorded position of the school from previous pings. The blind zone is marked with a 50 m white circle around the vessel origo, and the outer sector starts at 300 m range from the vessel. Any recieved echo beyond this point, are automatically neglected from the scrutinizing process. B) The LSSS map geographically displaying all sandeel school observations and their swimming direction.

2.3.4 Analyzing with LSSS and Korona

Echo sounder post-processing used conventional LSSS scrutinizing according to Korneliussen *et al*. (2006). The objective was to analyse the same area that were covered by the sonar (Hardangervidda and Østbanken) in order to compare the results and performance between the acoustic systems. The recorded frequencies for this survey were at 18, 38, 120 and 200 kHz. The data files were first pre-processed with Korona regions according to guidelines provided by Korneliussen *et al*. (2006). Pre-processing the raw files would remove visual noise and smooth the echogram display. A pre-configured Korona data training set were used to automatically define regions of sandeel schools from other fish backscatter. A regions is defined as an enclosed area where all values are equal to or above a certain threshold. All values outside the regions are below designated threshold and neglected from the results, but a selected region is allowed to have holes in it. The categorisation files used by Korona was collected from an installed version of LSSS used onboard Johan Hjort 2011 survey. The reflection properties of sandeel targets such as frequency response and target strenght was used to estimate a detection possability (%) for sandeel. Korona school recognition and identification of sandeel schools are further described by Mohammed (2006) and Johnsen *et al.* (2009) where former sandeel experiments has provided three different frequency responses utilized on this scrutinizing process (Fig. 16). The frequency response *r* (*f*) is defined by Johnsen *et al.*(2009) as the ratio between the mean area backscattering coefficient $<s_A>$ (m^2/nmi^2) at a given frequency and the "reference frequency" measured at 38 kHz . Normalized by the mean $<s_A>$ for the four applied values of frequencies in the school region, the proportional frequency response r(*f*) is defined as

$$r(f) = \frac{s_A(f)}{s_A(38)} \quad . \tag{22}$$

A "flat" frequency response on a school target then means that the echo from the school is the same at all frequencies. For sandeel (Fig. 16) the echo is relative weak at the lowest frequency, 18 kHz and rapidly rising at 38 kHz. Further, depending on the size of the

individual sandeel inside the school, it is either gradually increasing with increasing frequency for small, 1 year old sandeel, but more flat, even dropping at 200 Khz for the larger 3 year old sandeel. As sandeel sizes swim in size specific schools, Johnsen *et al.* (2009) found that it was possible to use the frequency response to discriminate not only between sandeel, herring and mackerel, but also between 1 and 2 year old sandeel.

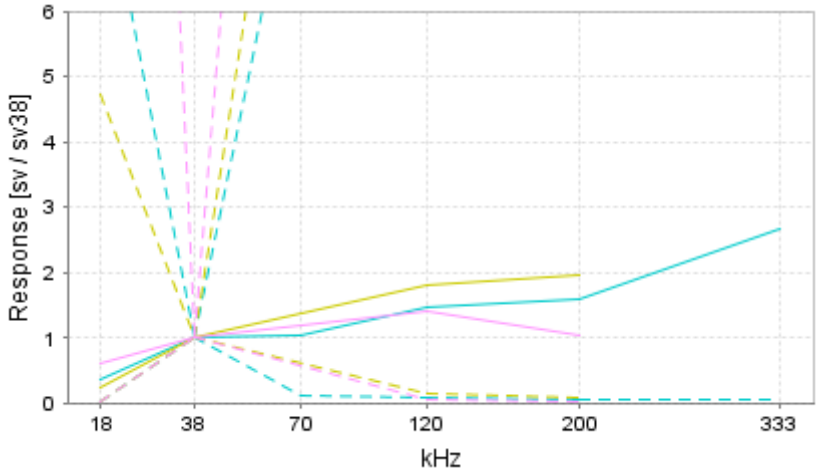

Figure 16. Three different frequency response curves of sandeel from the Korona categorization library. The response curve repressent data from different size groups of sandeel. Stippled lines represent confidence intervals .For this particular survey only 18, 38, 120 and 200 kHz were utilized.

By implementing frequency response data together with knowledge of the distinct sandeel schooling shape and size, the scrutnizing process was conducted with relative high precision. Each sandeel schools scrutinized with Korona was assigned to a category and ID with corresponding school parameters. Height, lenght, cross sectional area and perimeter values of every detected school was calculated by Korona and exported to a database (Fig. 17). For parameter details, see Korneliussen *et al.* (2009). The overall information of school dimensions from EK60 and SH90 was compared with each other from recorded time logs and geographic coordinates. Recorded backscatter used for biomass estimation $\langle s_A \rangle$, is the scaled area backscattering coefficient [m^2/nmi^2] for # nautical miles. (MacLennan *et al.*, 2002) With latest knowledge regarding sandeel target strength (TS), we have used the suggested lenght-TS relationship (Kubilius *et al.*, 2012),

$$TS = 20\log L - 93.1\ dB \quad . \tag{23}$$

The backscattering cross section $<\sigma>$ $(4\pi 10^{(TS/10)})$ was estimated from mean TS at sandeel length L. The number of sandeel (N) for each school was estimated from the average of the area backscattering coefficient, $<s_A>$, divided with average backscattering cross section, $<\sigma>$, and multiplied with the estimated school area (A_S),

$$N = \frac{<s_A>(f)\,A_S}{<\sigma>} \quad . \tag{24}$$

Assuming that school lenght (L_S) is the same as width, the cross sectional area may be defined as

$$A_S = L_S \cdot L_S \quad . \tag{25}$$

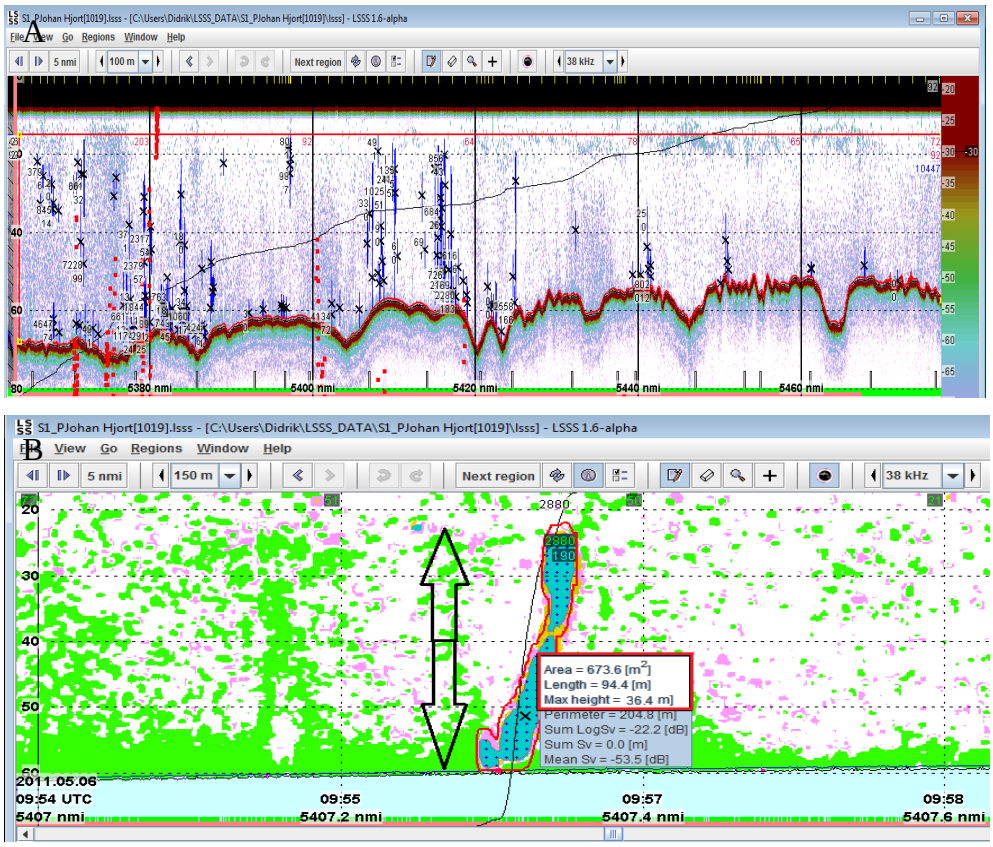

Figure 17: A) LSSS echogram screen displaying all scrutinized sandeel school from Hardangervidda. B) The height, lenght, area and other parameters are meaured by Korona. Mean $<s_A>$ (also referred to as nautical area scattering coefficient (NASC)) and mean $<s_V>$ derives from the averaging the backscatter inside the school boundary.

3. RESULTS

3.1 Catch and biological data.

Sandeel measured in body length and weight were sampled by dredge and bottom trawling at various points during the survey (see 2.1.1) and measured by the IMR technical staff. The length and weight distributions are showed in Fig. 18 with samples taken from the survey sites Inner Shoal East and Hardangervidda respectively. The mean length from Inner Shoal East was measured to 14.0 cm with 95% confidence interval between 13.8 and 14.3 cm. The mean weight was 10.3 g with 95% confidence interval between 9.9 and 10.6 g. Mean length from Hardangervidda was measured to 15.7 cm with 95% confidence interval between 15.5 and 15.8cm, with mean weight was 14.9 g with 95% confidence interval between at 14.5 and 15.3 g.

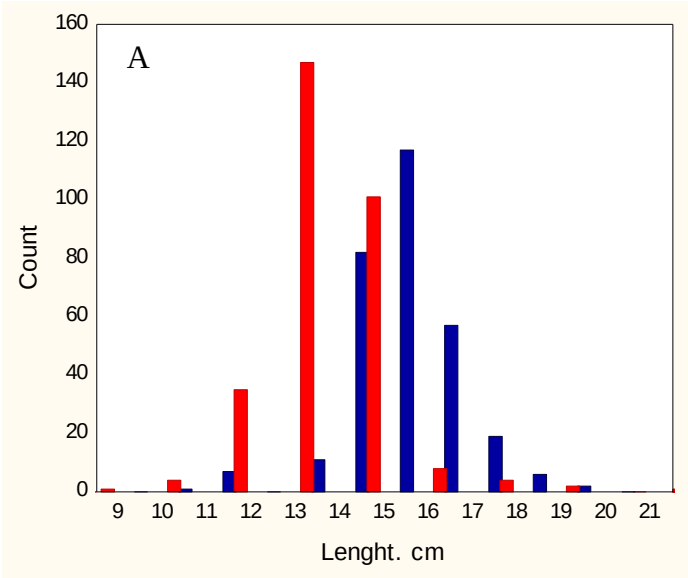

B	Inner Shoal East	Hardangervidda
Nr. of samples	302	303
Mean lenght (cm)	15.7	14.0
Std Dev length	1.2	2.1
C.I. of Mean length (cm)	0.14	0.24
Mean weight (g)	10.3	14.9
Std Dev weight	2.7	3.6
95% C.I. of Mean weight	0.3	0.41

Figure 18. A) The length distribution of sandeel estimated from bottom trawl and dredge catches from the Hardangervidda bank (red) and Inner shoal east bank (blue). B) Table showing the number of samples taken from each survey ground of sandeel weight and length. Descriptive statistics is mean length and weight, the standard deviation and 95% confidence intervall of the means.

3.1.1 CTD data

CTD casts were taken during the survey with 6 measurement stations from Inner Shoal East and 8 from Hardangervidda. CTD transect from Inner Shoal East (Fig. 19) was created from a 42.5 nmi long transect between longitude 3.1397-5.0112 E, and latitude 56.6388-

57.4982 N with 449 measurements composed from 6 stations. The average depht was measured at 31.1 m with standard deviation 16.7 m, the maximum measured depht was 80 m. Average temperature was measured at 6.538 ° C with standard deviation at 1.017 °C, maximum and minimum temperature was measured at 8.893 and 5.625. Average salinity was measured at 35.038 PSU with standard deviation of 0.03, max and min value was measured at 35.138 and 34.983 PSU. Average sound velocity was measured at 1480.23 m/s with standard deviation of 3.136 and max/min values of 1485.97 and 1475 m/s. CTD casts taken from all survey points show a weak thermocline around 15 meter for both areas (Fig. 19). CTD transect from Hardangervidda was created from a 47.5 nmi long space between longitude 2.7883 – 6.4433 and latitude 56.6388 - 58.164 with a total of 257 measurements composed from 6 stations. The average depht was measured at 28.7 m with standard deviation 15 m and maximum depht at 57 m. The average temperature was measured at 6.81 °C with standard deviation 1.028 °C, max/min temperature was measured at 8.435 and 6.0 °C respectively. Average salinity was measured at 34.834 PSU with standard deviation of 0.04 and max and min value of 35.072 and 34.63 PSU. Average sound velocity was measured at 1488.47 m/s with standard deviation of 1.451, max and values of 1484.95 and 1480 m/s.

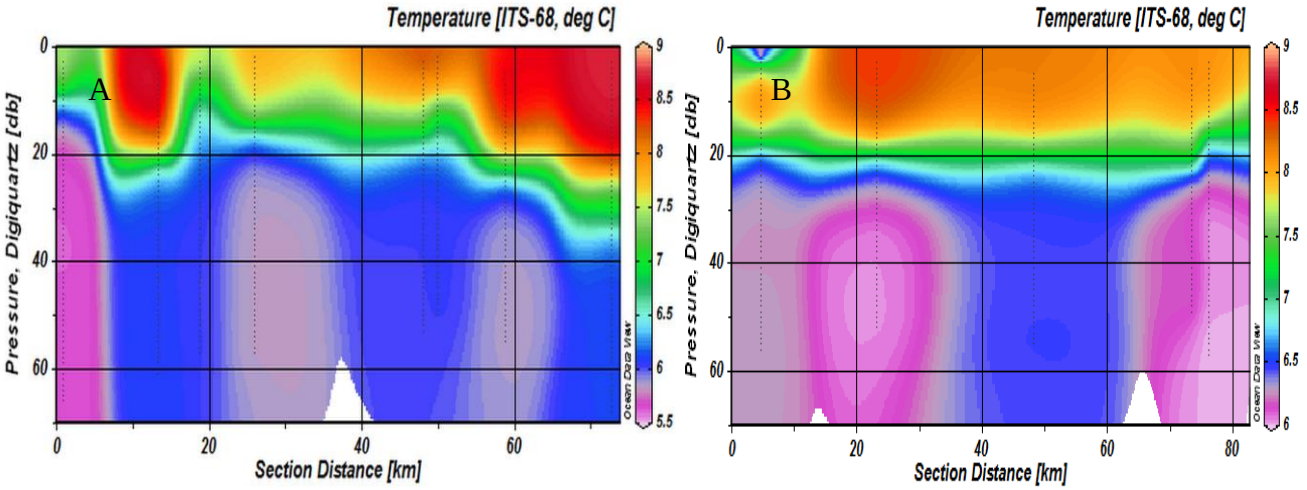

Figure 19. A) Inner shoal east CTD temperature transect. B) Hardangervidda CTD transects. Temperature range is between 9 and 5.5 °C for both banks. (CTD transect created by Ocean Data View 4)

3.2 Meaured schools from ImageJ

ImageJ analyses of sandeel schools from the sonar display screenshots are presented below in Table 4. The data was sampled from the total number of manually recorded school observations (750 schools) from the entire survey period. The measured school parameters were areal size, max width and max height, school perimeter, perpendicular range and angle of school relative to the vessel heading. All school detections distributed from the sonar display according to their corresponding range and angle are displayed in Fig. 20 A. The results show that the sonar is able to detect schools at any point in the range beetween 50-290 m with mean range at 170 m. The schools are distributed in the whole circular range between 270 – 180 degrees with most detection made in front of the vessel in the sector covering 300 to 60 degrees. The sonar's vertical display occupied the screen angle between 180-270 degrees during most of the surveying time, which explainis the lack of targets in this particular part of the display (Fig. 20 A). The number of counted schools is displayed from the survey period of 15 days (24.04 – 07.05.2011) with areal size vs number of observations. (Fig. 20 B)

Table 4: Measured school parameters of 750 school observations. The parameters is measured mean value with standard deviation, standard error, 95% confidence interval of mean, max/min value and 25% and 75 % percentiles.

	Mean	**Std Dev**	**Std. Error**	**C.I. of Mean**	**Max**	**Min**	**25 %**	**75 %**
Area (m^2)	1225.1	1212.3	44.3	86.9	7178.5	41.1	397.9	1656.8
Perimeter ($m^)$	252.1	174.0	6.4	12.5	1311.2	31.1	129.0	323.6
Width (vector x) (m)	53.3	30.0	1.1	2.2	183.5	7.1	30.5	67.7
Height (vector y) (m)	44.3	24.2	0.9	1.7	145.9	4.2	26.5	58.0
Angle of school to vessel (°)	77.9	56.8	2.1	4.1	178.2	-172.4	52.8	119.0
Range from vessel (m)	170	61.4	2.2	4.4	300.1	20.4	118.0	221.1
Corrected width (m)	42.4	24.2	0.9	1.8	144.1	3.2	24.7	55.7
Corrected height (m)	35.7	26.2	1.0	1.9	163.3	0.08	17.3	48.3
School diameter (m)	35.5	17.3	0.6	1.2	95.6	7.2	23.6	45.9

One of the most important parameters from the data set was the measured school area. The measured average school area from the results was 1226 m^2, 95% confidence intervall of this value was measured at 86.9 m^2. This parameter was converted to logharithmic values, in

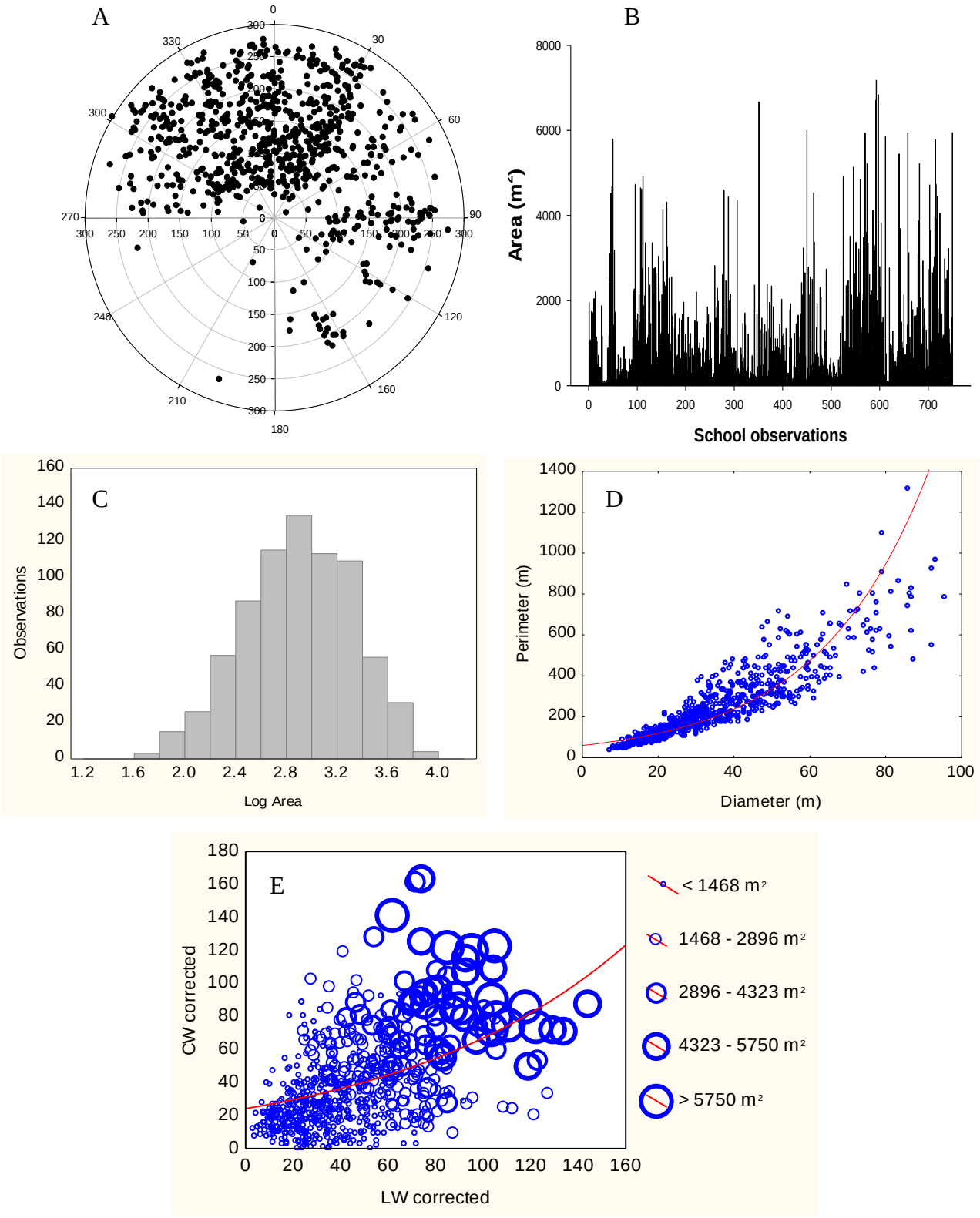

Figure 20. A) Total number of school detections in relation to range and angle on the sonar display. B) Total number of recorded schools with corresponding area chronological distributed over the survey period. C) A normal distribution of logarithmic converted values of the school area, together with number of observations. D) Scatter plot of school perimeter over school diameter. The regressional fit shows an exponential increase of the perimeter as function of diameter. E) Scatter plot of observed school area (m^2) where circle size corresponds to the area class over corrected width (LW corrected) and height (CW corrected) in meters.

order to be tested for a normal distributed fit with Statistica (Fig. 20 C). A Chi-Square normal specific distribution test with 95% confidence intervall showed a value of 15.95 with 8 freedom degrees (*df*), this provided a significant p-value of the confidence intervall (0.95) where $p < 0.043$. The more powerful Shapiro-Wilkinson normality test accepted the distributional fit when $p = 0.00137$, even if this test is considered more suitable for larger data samples (N>5000). Measured school parameters diameter, corrected school lenght and width were estimated from the circular radius (eq. 19), and beam width correction (eq. 20; 21). The relationship between areal size between school lenght/height and areal size (Fig.20 E), show decent correlation with expected areal values. The relationship between estimated school diameter and measured perimeter (Fig. 20 D), show a correlated exponential fit with for the smaller schools with regressional function $LOG(perimeter) = 1.246 \cdot LOG(diameter) + 0.441$.

3.3 Measured schools from PROFOS and LSSS

Results from scrutinized raw data from the two sandeel banks Hardangervidda and Inner Shoal East are divided in two parts. The first one compare detection performance between the two acoustic systems, the second part compare the sandeel school parameters beetween acoustic systems. The covered transects from each bank was at similar lenght with 103.5 nmi covered for Hardangervidda and 112.5 nmi covered for Inner Shoal East. Fig. 21 shows the number of observed schools for each of the acoustic systems over covered distance (nmi) at the two banks. It is possible to observe an interspecific trend between observations from the acoustic systems. Hardangervidda showed similar detection frequency on both instruments along the transect. However, Inner Shoal East had a section (74.1 - 112.5 nmi) where sonar observations largely deviated from the echo sounder observations, and the detection ratio R was 2 observations against 56 (0.04). Total number of counted schools had relationship 0.57 for Hardangervidda and 0.16 from Inner Shoal East with an average school density for each bank estimated at 25.9 and 9.6 schools/nmi^2 respectively. Table 5 shows descriptive values for each bank, splitted in to three relative equal sized strata. The number of detected schools is extrapolated with their respectable survey area in order to estimate the school denisty per nmi^2.

The survey area for each stratum was estimated from the relationship between the covered transects lenght and DC when CV is assumed to be around 20%. (See eq.10). The

largest density of observed schools with the sonar was 75 from stratum 3 and smallest oberved schools were 7 from stratum 3 at Inner Shoal East. Largest density of observed schools with echo sounder was 43 at stratum 1, while smallest observed density was 1 school from stratum 3 at Hardangervidda. The largest deviation between the two acoustic systems was both found in stratum 3 from Inner Shoal East and Hardangervidda with detection ratio 5:75 and 1:15 respectively. The smallest detection deviation between the two acoustic systems was found in stratum 2 Inner Shoal East were the ratio was 8:7. Wilcoxon matchet pair test and conventional paired t-test for both banks (total survey areas), showed significant difference between the recorded school density ($p < 0.05$).

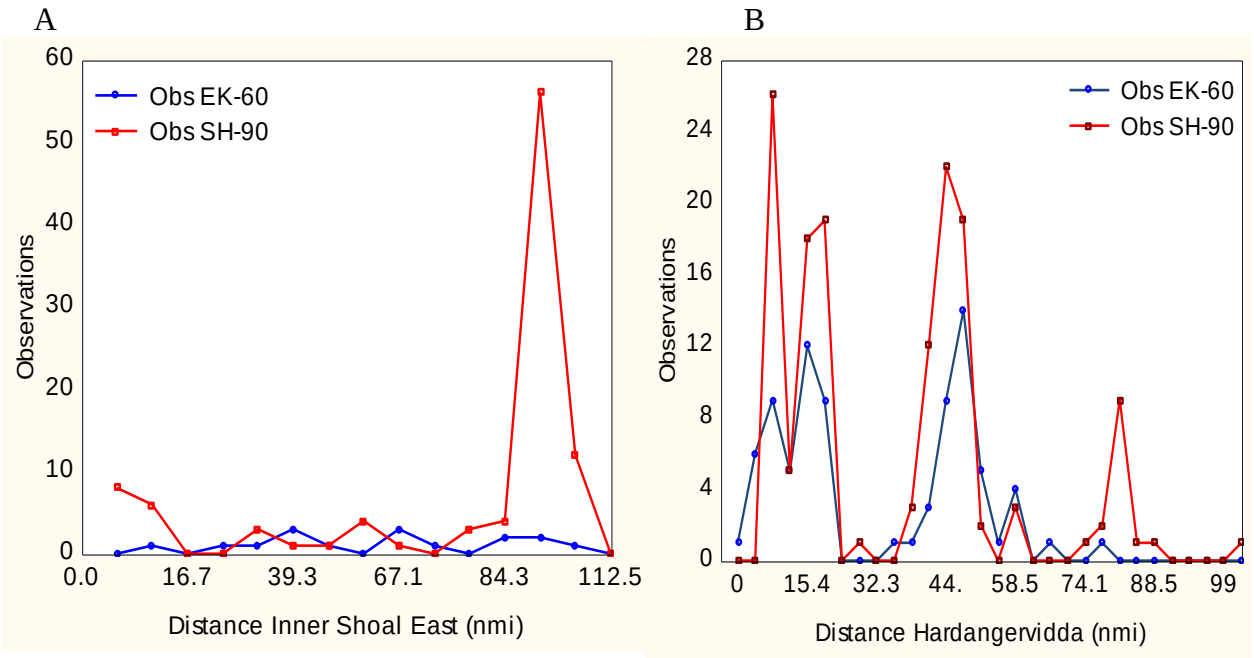

Figure 21. A) School observation plot from Inner Shoal East displaying total sandeel recordings from sonar (red) and echo sounder (blue). Number of detections are quite low for both systems whereas the section beetween 74.1 to 112.5 nmi the sonar detected 75 schools and the echo sounder detected 5 B) School observation plot from Hardangervidda shows the distribution of schools across the transect. The distribution over time was similar for both acoustic systems where the sonar had an average of 1.77 times more school detections compared to the echo sounder.

Table 5: School observations from the two sandeel banks divided in to substrata and total survey area. L: transect lenght i nmi. N_E: recorded observations for the echo sounder. N_S: recorded observations for the sonar. $N_E/N_S/nmi^2$: average school density of nmi^2. R: fraction of recorded schools with echo sounder (N_E/N_S).

Inner Shoal East	**L (nmi)**	**Area(nmi^2)**	**N_E**	**N_S**	**N_E /nmi^2**	**N_S/nmi^2**	**R**
Stratum 1	33.8	29.5	3	17	0.5	12.7	0.18
Stratum 2	40.3	41.5	8	7	1.3	1.1	1.14
Stratum 3	38.4	38	5	75	0.8	12	0.08
Total survey area	112.5	350	16	99	2.7	16.5	0.16
Hardangervidda	**L (nmi)**	**Area (nmi^2)**	**N_E**	**N_S**	**N_E /nmi^2**	**N_S/nmi^2**	**R**
Stratum 1	33.4	28.5	43	69	6.9	11.0	0.62
Stratum 2	39.04	39	38	61	6.1	9.8	0.62
Stratum 3	31.06	24.7	1	15	0.2	2.4	0.07
Total survey area	103.5	300	82	145	13.7	24.3	0.57

3.3.1 School size distribution

The measured school area from EK60 and SH90 observations was accumulated from both survey areas in order to facilitate a more comprehensive data set. Total observations from both banks were 101 schools from EK60 and 244 schools from SH90. Average school area measured by EK60 was 248.3 m^2, 95% confidence of the mean was 215.3 and 281.1 m^2 with standard deviation 166.5 m^2. The largest and smallest measured school from EK60 was 752.8 and 67.5 m^2 respectively. Average school area measured by SH90 was 1325.5 m^2, 95% confidence intervall of the mean was 951.5 and 1325.5 m^2 with standard deviation 1452.8 m^2. The largest and smallest school area measured from SH90 was 60.4 and 11873.9 m^2 respectively. The distribution of area size resembled the data set from Image J with a chi-square fit for lognormal values showing ($p < 0.05$). Fig. 22 show two images representing the relationship between cumulated detections from EK60 and SH90 schools, ranked from smalles to largest size. Areal distribution of recorded EK60 schools showed that 28% of the total number of observations was found in the range between of 60 – 750 m^2. The smallest schools were found between the area classes 60-230 m^2, EK60 recorded schools represented here 19% of total obervations, compared to 6% from the SH90. Table 6 show the average depth in the water column and biomass of individual schools estimated from EK60 within their area class and mean area backscattering coefficient, $<s_A>$. Average sandeel lenght and weight samples used to estimate the biomass was taken from their respectable trawling sites.

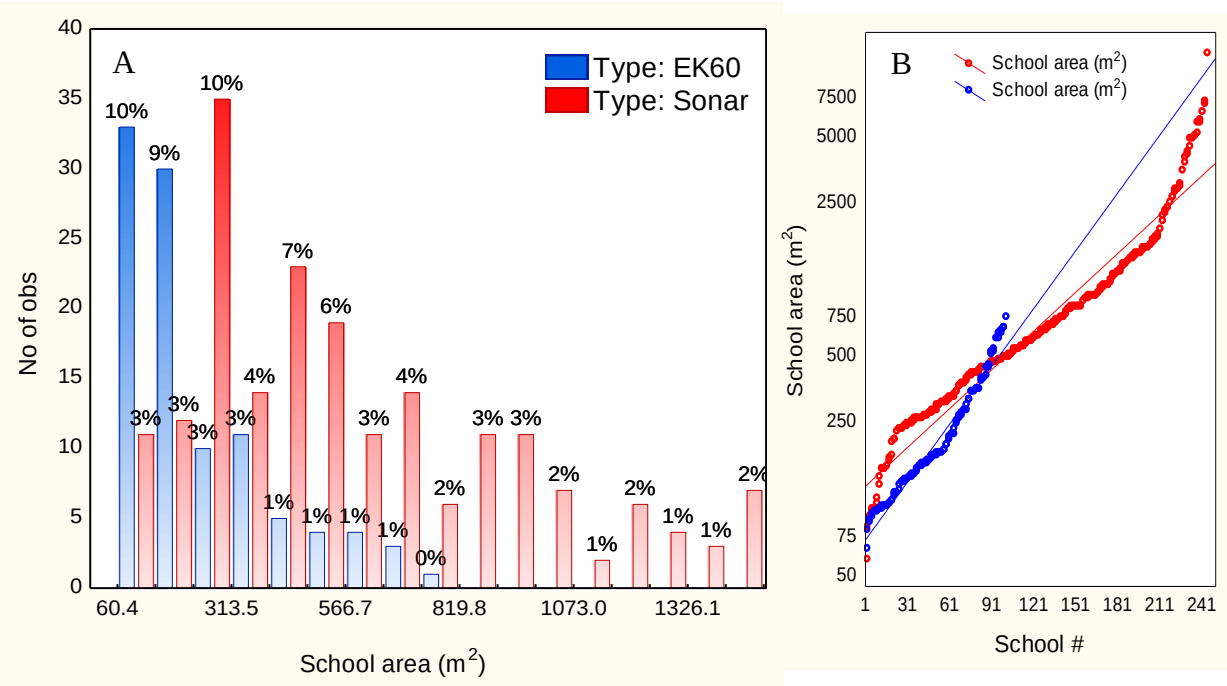

Fig. 22. A) The cumulated sandeel observations from EK60 and SH90 size distributed in a histogram with percentage bars. B) Log scaled cumulative line plots beween EK60 and SH90 school area ranked after size.

Table 6. The relative biomass of two school size distributions. Areal sizes of 68 to 236 m^2 represent 6% of cumulative SH90 observations compared to 19% from EK60. Areal class beetween 249 to 753 m^2 represent 34% of SH90 observations and 10% from EK60. Any school size beyond 753 m^2 where only detected by SH90. Average depth is the location of schools in the water column detected by the echo sounder.

School size	N	Mean tons	Minimum	Maximum	Std. Dev	SH90 fraction	Average depht
68-236 m^2	63	2.48	0.17	9.31	1.88	< 6%	43.2 m
249-753m^2	37	17.10	1.05	78.52	19.01	>34%	33.8 m

3.3.2 EK60 vs SH90 school size comparison

When comparing recording time and digital coordinates on school observations in PROFOS and LSSS, which schools were most likely to be detected on both the sonar and echo sounder display could be estimated. These schools naturally needed to be detected straight in front of the vessel on the sonar. The number of direct comparable schools was 29 from Hardangervidda and only 5 from Inner Shoal East. For a simpler data set, all recordings were merged into to one, and Fig. 23 display the selected schools compared. Since the echo sounder can only detect the vertical cross section of schools, the perpendicular area were estimated from the assumption that school lenght is the same in

both directions ($A_S = L_S \cdot L_S$). The results show that the sonar beam may detect larger, smaller or even equally sized schools compared with the estimated area from the echo sounders more narrow vertical beam. School sizes estimated from sandeel lenght (L_S) in the size class (400-2220 m^2) were underestimtated on 13 of the measured shools and overestimated for 5 schools. The larger size class however (2200-14000 m^2), was undertimated only for 3 schools, while overestimated for 9 shools. Schools that measured an approximate equally by the two acoustic systems were school nr. 8, 33, 32, 7, 12, 18 and 23. The average school area from EK60 detections was 3250.1 m^2 for EK60 schools and 3154.2 m^2 for SH90 schools. The fractional size of echo sounder schools is overestimated 1.7 times in average of the sonar area. The measured mean of relative school volume, estimated from the sonar school area (A_S) and from school height (H_S), was 38 083 m^3. Summary of descriptive statistics of sandeel comparison with are displayed in Table 7.

In two occations during scrutinizing, the sonar detected one school at the same point as the echo sounder recorded two nearby independent schools (school # 10-11 and 20-21). The challenge was solved by allocating a school ID each school and use the same area from SH90 recordings for further school comparisons. The biomass for each individual school was estimated from its mean area backscattering coefficient $\langle s_{A} \rangle$ and multiplied with its relative area in nmi^2 from school lenght (L_S), (See eq. 25). Fig. 23 shows the scatter plot between estimated biomass of schools with relative volume volume and measured area.

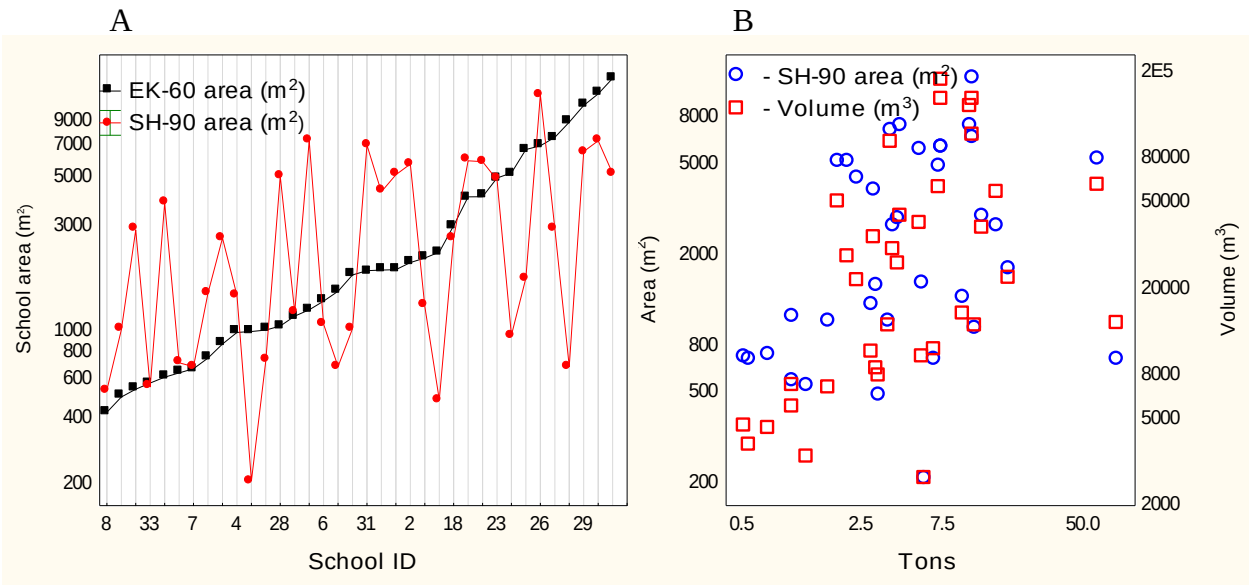

Figure 23: A) Area plot of sandeel schools ranked after size with ID tags (#). School 1 -31 is compared from Hardangervidda, and school 32 -36 is compared from Inner Shoal East. (B) Scatter plot of measured school area from sonar (blue circles) and estimated school volume (red squares) over biomass (tons).

Table 7: Descriptive statistics of the 36 sandeel schools measured by both acoustic systems. Mean: The average value of measured parameter. C.I ± 95%: the confidence limits of mean. Std.Dev: the standard deviation of samples. SE: the standard error of mean.

Summary sandeel comparison (N=36)	Mean	C.I -95%	C.I 95 %	Std.Dev	SE
Mean Area SH90 (m^2)	3154.2	2216.9	4091.5	2770.2	461.7
SH90 school diameter (m)	57.3	48.0	66.6	27.4	4.6
Area EK60 (m^2)	3250.1	2049.0	4451.2	3549.8	591.6
Lenght EK60 (m)	50.3	41.1	59.5	27.2	4.5
Fraction area (EK60/SH90)	1.7	0.9	2.5	2.4	0.4
Height EK60 (m)	11.8	9.7	13.8	6.1	1.0
Volume of school (m^3)	40464	24410	56519	47449	7908
Diameter EK60 (m)	56.8	46.4	67.2	30.8	5.1
Biomass per school (tons)	9.25	3.95	14.55	15.66	2.61
Volume density per school (fish/m^3)	33.5	10.4	56.6	68.3	11.4
School depht (m)	34.0	29.8	38.3	12.6	2.1

3.4 Survey distribution and biomass estimation.

The abundance in each survey area was estimated with an assumed relationship between the coefficienct of variation (CV) and the degree of coverage (DC) of 20% for both banks. The Inner shoal east was 350 nmi^2 and Hardangervidda 300 nmi^2. The average sandeel school diameter of 35.5 m was measured from the ImageJ data set and used to estimate the detection probabilty for the EK60. The effective detection width for the sonar was estimated to be about 480 m, from evaluations made in Lybin, using the sound propagation conditions and the bottom depth as input parameters, but also the backscattering of sandeel scools. The echo sounders detection width for Inner Shoal East, was estimated to be 46.7 m at a mean depth of 50 m when the mean school size and the beam width was used in the evaluation. Similarly, the detection width for EK60 from Hardangervidda was 48.9 m at a mean depth of 60 m. The school detection probability for both acoustic surveys were incorperated to each surveyed transect to estimate the relative DC and CV according to their respectable survey area (Table 8).

Most recent data regarding sandeel TS-lenght relationship was TS= 20LogL -93.1 (Kubilius *et al.*, 2012), provided a mean backscattering cross section of $\langle\sigma\rangle$ = 1.211E-06 (m^2) from Inner Shoal East and $\langle\sigma\rangle$ = 1.366E-06 from Hardangevidda. The measured accumulated area backscattering coefficient $\langle s_A \rangle$ from each bank was divided by echo sounder school observations (N_E), for estimating the average school biomass in tons. A simple

biomass estimation with the sonar recordings was done by multiplying the average sandeel school weight from echo sounder recordings with the number of recorded sonar schools (N_S) from their respectable area. Fig. 24 and Table 9 show the estimated biomass from each survey area. The results show that Hardangervidda had a significantly higher density compared to Inner Shoal East. Interspecific comparison between the acoustic systems show that sonar detection width for sandeel may alone increase the degree of coverage (DC) with around 52.0 unit of effort, depending on bottom depth, from an initial survey coverage of 6.16 and 6.0 respectively. The relative gain in biomass by use of sonar alone Inner Shoal East may potentially increase with a factor of 5 times the amount recorded with the echo sounder, and 1.7 times the amount in Hardangervidda.

The sample CV (Table 8) is defined as a proportion, $CV = s/\overline{N}$ where s is the standard deviation, and $\overline{N}$ is the sample mean. The unit is a measurement of the relative sampling precision, which is invariant to scale changes (but not location change). All the samples from the sonar were manually implemented in the scrutinized LSSS survey report and counted together, with 0.1 nmi resolution scale with: x = number of sandeel school(s), and 0 = density zero.

Table 8. Distribution of effort (DC) between relative detection widths, of the two acoustic equipments. For biomass estimation, the measured $<s_A>$ (nautical area backscattering coefficient) is used from each bank. Average school $<s_A>$ is estimated by scrutnized sandeel $<s_A>$ divided by school observations (N) for the two acoustic systems. Coefficient of variation (CV) on sample density is estimated from standard deviation of school observations, divided by mean school count along the transect. The school counting from sonar and echo sounder was done manually with 0.1 nmi resolution.

Survey Effort	**Inner Shoal East**	**Hardangervidda**
Survey Area (nmi^2)	350	300
Average depht (m)	50	60
Covered area with EK60 detection width (nmi^2)	2.8	2.7
Covered area with SH90 detection width (nmi^2)	27.3	26.8
Degree of coverage with EK60	6.01	5.98
Degree of coverage with SH90	57.8	58.6
CV survey effort EK60 (%)	20.4	20.5
CV survey effort SH90 (%)	6.6	6.5
Biomass estimation		
Sandeel $<s_A>$ (m^2/nmi^2)	4.01	61.10
Average school $<s_A>$ ($m^2/nmi^2/N$)	0.21	0.75
CV of sample density EK60 (%)	347.9	336.0
CV of sample denisty SH90 (%)	440.6	368.7

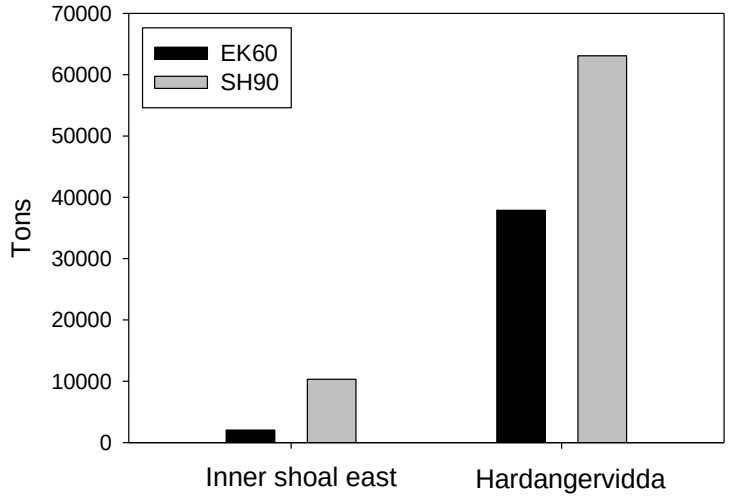

Figure 24: The estimated biomass of each bank from echo sounder data and sonar recordings.

Table 9. The measured biomass of Inner shoal east with echo sounder was 2049 tons when extrapolated with the survey area of 350 nmi^2. The increased detectional swath width of the sonar would increase sample precision (CV) by 26.7 %. The survey effort from the sonar measured 10 315 tons of relative biomass, an increase of 403% compared by the echo sounder. Hardangervidda measured 37 876 tons when extrapolated with the survey area of 300 nmi^2. The increase of sample precision (CV) with sonar was 9.7 %. The releative biomass recorded from sonar recordings was 63 076 tons, an increase of 66.5%, compared to the echo sounder.

Inner shoal east	**Detection swath width**	**N**	**Estimated biomass**
EK60	46.7 m	20	2049 tons
SH90	480 m	99	10315 tons
	Sample precision (CV) increase	**N/nmi^2**	**Potential increase in tons**
EK60	-	3.3	-
SH90	26.7%	16.5	403.42%

Hardangervidda	**Detection swath width**	**N**	**Estimated biomass**
EK60	48.9 m	82	37876 tons
SH90	480 m	146	63076 tons
	Sample precision (CV) increase	**N/nmi^2**	**Potential increase in tons**
EK60	-	13.7	-
SH90	9.7%	24.4	66.5%

4. DISCUSSION

This study reveals that estimating the correct sandeel density with omnidirectional sonar is a challenging task, where both acoustic systems give an estimate of biased fish densities due to equipment limitations. The potential gain by using sonar in acoustic surveys, possible sources of errors and challenges on collecting data with sonar are discussed below.

The large sampling volume of the sonar enables an increased sampling intensity compared to conventional echo sounder surveys. The continuous data recording enables an evaluation of sandeel density with spatial structure of schools on the field (Fig. 8). This experiment was tested during summer in shallow water (40-60 m) where CTD results showed no significant temperature oscillations. The effective covering range of sonar would in this case be estimated to around 250-300 meter using -6° beam tilt with the Lybin programme (Fig. 11).

The detection swath width for sonar for weak schools was estimated to be about 480 m, compared with the echo sounders approximately 50 m, and the sampling intensity would theoretically give an increased detection ratio of 9.6. However, the results show that recorded sandeel density with sonar only increased with 1.44 and 3.02 times for Hardangervidda and Inner Shoal East respectively. This small increase is due to the fact that sandeel schools are relative large when the mean measured area of 750 schools was 1225 m^2. (Table 4) The chance of such schools being hit by the echo sounder on a field would therefore significantly increase, and it will increase proportionally with the school width. In terms of detection ratio, the results show that the increased covering width of the sonar would not synonymously increase proportionally. However, the sonar performed better on detecting schools over the low density bank Inner Shoal East, where it was capable to detect rather large school clusters were the echo sounder did not (Fig. 21 A). In surveying of patchy distributed fish this is quite important, since areas with schools may easily be missed with the narrow echo sounder beam. The smaller the schools, the larger are the chance of missing registrations on the echo sounder.

The sonar detection ability is mainly determined by the increased covering width and the difference in detection treshold. In order for a school to be optimally hit by the sonar beam, the schools have to be located above a certain vertical limit in the water column (Fig. 6). Table 6 show the average depht of 43.2 m, measured from echo sounder of smallest set of schools, while the larger size class was measured at 33.8 m. This suggests that smaller schools are generally deeper and situated closer to the seabed compared to the larger and taller

schools. Sandeel are known to be quite distinct in their school shape for being slim and tall (Mackinson *et al.*, 2005), and the probability for the upper part of the school being hit by the horizontal sonar beam would increase with its size. In Fig. 22 we can observe the detection frequency of ranked school sizes. The sonar is able to detect school of all sizes but with a much lower frequency in the size class of 60 to 230 m^2. The smallest schools recorded by both acoustic systems represented 25% of total sandeel recordings while the sonar system neglected these with approximately 31.6% of total sandeel recordings. The echo sounder recordings were characterized by a few very large and many medium-sized to smaller schools, where the latter accounted for most of the biomass, the sonar would mostly record medium sized to larger schools. The average biomass of smaller schools (70-240 m^2) was estimated around 2.5 tons while larger schools (240-750 m^2) had larger biomass with estimated average at 17.1 tons. However, the cumulative biomass of the small schools may significantly reduce the biomass abundance if it would be removed from a potential acoustic survey with only the sonar in use.

Results from Fig. 23, show that the narrow swath width of the echo sounder would at most instances underestimate the true value of school size. The number of comparisons made between schools, was relative small due to few occasions where the detected schools would pass under the vessel. This may suggest that the relative small schools may contribute a significant part of the total biomass due to only a part of the school being hit by the vertical beam. For the sonar system, the backscattering intensity from the smallest schools is often masked by surface clutter and bottom reverberation in shallow water, and the relative echo intensity of such schools has to exceed a certain treshold in order to be detected. The largest school areas estimated from the echo sounder was more frequently overestimated compared with the sonar. On the horizontal plane, larger schools are sometimes elongated with one long and one slim side. It is therefore likely that the echo sounder could have covered a few such large schools along it full length. In a potential biomass estimation survey, this would be a source of error on the estimated NASC value, while the overall averaging would reduce this effect. If the sandeel schools are not spherical on cross section, this may explain some of the differences between the area measured by the two systems. The scatter plot of school perimeter over school diameter (Fig. 20D), suggests that the largest schools are less spherical in shape compared to the smaller schools. The area of eliptical or elongated schools will by the echo sounder be underestimated in most crossings, unless the school is hit and passed in the longest direction. So the probability of underestimation the area with echo sounder is larger than the probability for overestimation of the area for such schools. (Fig. 23A).

The biomass estimation from sonar recordings were simplified by using the average school backscattering from the EK60 recordings (Table 9), and the relationship between number of schools as a dependent variable and estimated biomass, was therefore quite linear. Fig. 24 show the potential difference of sandeel biomass that may be missed by the echo sounder. With the same survey effort, the sonar conducted survey have a potential for a significant increase of biomass. The level of sonar sample precision (CV), where a high CV value reflects inconsistency among the samples within the sandeel bank, some, but not a very large gain in CV can be expected (Table 8). Hardangervidda would increase with 9.7% over the echo sounder, while the low density area Inner Shoal East increased with 26.7%. This deviation is mainly determined by the distribution of sandeel on the field. The echo sounder would detect small schools relatively consistent trough the survey, while the sonar was better at detecting larger school aggregations but with less frequent encounters.

When undertaking a survey design with sonar, the covering width of the sonar may alone reduce the amount of effort needed to achieve the desirable DC/CV relationship from the survey. But the relative gain is also determined by the mean school size, e.g. increased survey effort on large schools would not dramatically impact the sample precision. The initial survey effort with echo sounder could in theory be potentially reduced by over 85% with the sonar, and still achieve the same degree of coverage. However, this effect is unrealistic regardless of the scale change as the sampling effort equation is invariant to the different detectional performance between the two acoustic systems. When taking the known school size and distribution into consideration, a potential survey with reduced effort may give an accurate distribution of school clusters on the field, but with inaccurate density estimates due to the sonar's detection limitations.

From a potential adaptive choice, the areal picture of schools from the echo sounder would mostly correlate with the school distribution from sonar recordings (Fig. 21). For Inner Shoal East however, the distribution varied considerably between the log distance 74.1-112.5 nmi, where the sonar detected 6.2 times more schools compared to the echo sounder. In this scenario, a chief scientist should consider repeating that particular field a second time with the echo sounder, as in the socalled two-stage adaptive surveying (Simmonds and MacLennan, 2006). Until there is established a robust method for estimating sandeel biomass from sonar backscatter, a recommended procedure for future surveys with sonar would be:

- Reduction of survey effort to achieve an appropriate DC/CV relationship with respect to the sonars covering ability.

- The echo sounder should be used together with the sonar for estimating the sandeel density of smaller schools, due to the sonar detection limitations.
- Future surveys to be integrated in a two-stage adaptive system, where possible high density patches are surveyed a second time with more frequent transects.

The sonar processing of the acoustic signals have sources of errors in terms of the correct measurements of school sizes. Korneliussen *et al.* (2008) describes the complex variations of school lenght and depth related to beam width and various transducer positions on a moving vessel. An example is a large school that could occupy the entire part of one beam and a smaller part of another, and/or whether a large part of the school is positioned outside the beams central axis. Such issues would also apply with this sonar system. It is therefore likely that a large number of school distortions are present in this data set, even with the applied beam width corrections from Misund (1990) and Brehmer *et al.* (2007). A strict definition of the sonar effective range, to only include "completely" detected schools may help this issue.

According to Simmonds and MacLennan (2005), schools detected with a horizontal beam it is systematically overestimtated. This decreases as the horizontal dimension of the school becomes smaller relative to the beam width. Misund *et al.* (1995) describes a technique to estimate the correct school area (A) from recordings with multiple sets of range (R). Initially, the apparent school width is recorded as the full distance across all beams intersecting the school. The true width however, is less than that, and as a distance it is proportional to R. With multiple measurements of area and range of the same school, a linear regression $\sqrt{A_R}$ can be estimated and extrapolated to apply for all measurements of A. (Simmonds and MacLennan, 2005). A similar attempt was made for this data set, but with unsatisfactory results. The regression technique described by Misund (1995), assume that all schools decrease proportionally according to R. Results from this survey however, show that the majority of recorded schools showed little correlation regarding A as a function of R.
A likely explanation for this is the school being fully or partially hit by the sonar beam, which is determined by the positional depht of the school according to the transmitted beam pattern. A typical example is a school detected at range point R_1, then to increase at its full areal extent at closer range R_2, and decrease again at R_3, eliminating any linear correlation beetween range and area. During the scutinizing process, the best effort on this challenge was to measure all school shapes at maximum size within the optimal range of the sonar (Fig. 8). This was done to ensure that most of the school was fully hit by the beam. Beam width

corrections for the lenght and width of the schools were then applied on the data set during the analysing procedure. Regarding further work with sonar school parameters, it is recommended that the relative size of sandeel schools require special attention.

Scrutinizing with PROFOS proved several key challenges. For instant the volume backscattering coefficent $<s_V>$ to biomass estimates for this sonar system, requires modification of the standard s_V equation to incorperate with multiple beams. This task lies beyond the scope of this study, and with additional lack of beam calibration, all the recorded echo levels were discarded from further analysing. During the survey, schools were initially recorded from the assumption that all schools were sandeel. Though there was no quantified species scrutinizing process during analysing, unless some schools showed unusual high s_V that could indicate that herring was present. The species composition from LSSS results showed that mackerel and herring accounted for around ¼ of total biomass from both survey areas. According to Pitcher *et al*. (1985), mackerel will sometimes merge together with other schooling sandeel, and it is therefore likely that a few of the recorded sandeel schools is a mixture of both species.

The new file format derived from SH90 was neither optimized with the latest PROFOS version. This made scrutinizing time consuming due to a systematic switch of diplays beetween the vertical and horizontal transmission when played forward. The vertical transmission would in turn inflict each marked school with an overestimated seed point and merge together with other schools and bottom echo from neighbouring pings. The overestimated markings from each seed point would be manually erased during scrutinizing. This is not an optimal approach due to the potential prospect of making human errors when estimating school size by the visual eye. The eraser tool, which is similar to that from Microsofts Paint, proved that schools measured from PROFOS may frequently be under- or overestimated. Until the file format issue are sorted out, the marking of schools with PROFOS should be approached with discretion.

During scrutinizing, neighbouring schools would often merge or split with eachother at different times according to the vessel position. This provided a challenge regarding a school being connected with another or not. It was unclear whether this could indicate a behavioral reaction towards the approaching vessel, or it was two schools appearing as one due to sonar processing resolution. In general, schools showed no particular vessel avoidance during tracking of schools. However, the sonar system showed future potential for undertaking a behavioral study of sandeel school dynamics.

CONLUSIONS

1. Sandeel schools can be detected well with the Simrad SH90 omnidirectional sonar in good to fair weather conditions.
2. The effective detection range for weak schools in shallow water is about 250 m. (Lybin and practical exeperiments)
3. The school area, perimeter, shape and position relative to the vessel can be measured from sonar images and from raw data.
4. Surveying with sonar and echo sounder show that the effective detection with of the two systems depends on mean school size, and is estimated to be 480 m for sonar and 47-49 m for echo sonder at the depth of about 50 – 60 m
5. For sandeel, school identification must still be made with multifrequency echo sounder.
6. The potential gain in survey degree of coverage is less than expected from theory, due to the effect of school size, but a slight gain may be expected in coverage and in CV.
7. The sonar survey show examples of potential missing of schools on echo sounder transects, and have therefore the potential for being a good tool in future two stage adaptive surveys.

ACKNOWLEDGEMENT

This dissertation would not have beeen possible without the crucial help and support of many people.

I wish to thank, first and foremost, my supervisor Prof. Egil Ona (IMR) who with great encouragement and patience helped me with invaluable support and constant guidance during the entire preparation and writing process for this dissertation. I also wish to thank Egil Ona for giving me the opportunity to participate on the North Sea sandeel- and whale counting survey, and the research survey on the Beaufort Sea 2011. These are experiences that I will never forget.

PhD. Hector Peña is thanked for being my second supervisor, and for the great contribution on my work and helping me solve all the obstacles along the way.

All the people at my office is thanked for support and interesting conversations during my time at IMR, I especially thank Martha Uumati and Rokas Kubilius for constant encouragement and never backing away from my stupid questions.

At last I wish to thank my best friends and fellow students Henrik Rye Jakobsen and Kjetil Magnussønn Olsen for five long years together. Without your support I would not be in this position today.

REFERENCE

1. Abramoff, M.D., P.J. Magalhaes, S.J. Ram. "Image Processing with ImageJ". *Biophotonics International*. 11.7 (2004): 36-42.
2. Armstrong E., and J.I Edwards. "Target strength of sandeels". *ICES CM*. B:20. (1985): 5pp.
3. Aglen, A."Random errors of acoustic fish abundance estimates in relation to the survey grid density applied" FAO fish report. 300 (1983): 293-298.
4. Aglen, A."Empirical results on precision —effort relationships for acoustic surveys". Reliability of Acoustic Fish Abundance Estimates. Dr. scient. thesis, Department of fisheries biology, University of Bergen, Norway (1989): 79–106.
   Aglen, A. "Sources of Error in Acoustic Estimation of Fish Abundance." *Marine Fish Behaviour In Capture And Abundance Estimation, Fishing News Books*. 7. (1994): 107-129
5. Brehmer, P., T. Lafont, S Georgakaros, E. Josse, F. Gerlotto, and C. Collet. "Omnidirectional multibeam sonar monitoring: applications in fisheries science."*Fish and Fisheries*. 7. (2006): 165-179.
6. Brehmer, P., S. Georgakarakos, E. Josse, V. Trygonis, and J. Dalen. "Adaptation of fisheries sonar for pelagic fish school monitoring: dependency of the schooling behaviour on the 'fish finding' efficiency." *Aquatic Living Resources*. 20.4 (2007): 377-384.
7. Connors, M.E, and S.J Schwager. "The use of adaptive cluster sampling for hydroacoustic surveys." *ICES Journal of Marine Science*. 59. (2002): 1314-1325.
8. DuPaul, W.D, and R.J Smolowitz. "The Development of a Modified Sea Scallop Dredge." *VIMS Marine Resource Report*. 1. (2003): 9 pp.
9. Engås, A. "Near-bottom sampling with bottom and pelagic trawls." *ICES CM*. 15. (1987): 9 pp.
10. Foote, K. G., K.P. Knudsen, G. Vestnes, D.N. MacLennan, and E. J. Simmonds. "Calibration of acoustic instruments for fish density estimation: a practical guide." *ICES Cooperative Research Report*, (1987): 144. 69 pp
11. Foote, K.G. "Acoustic sampling volume." *Journal Acoustic Society of America*. 90.2 (1991): 959-964.

12. Foote, K.G., D. Chu, T.R Hammar, K.C Baldwin, L.A Mayer, L.C Hufnagle, and J.M Jech. "Protocols for calibrating multibeam sonar." *Acoustical Society of America*. 117.4 (2005): 2013-2027.
13. Freeman, S. M., S. Mackinson, and R. Flatt, "Diel patterns in the habitat utilisation of sandeels revealed using acoustic survey techniques". *Journal of Experimental Marine Biology and Ecology*, 305. (2004): 141–154.
14. Greenstreet, S., E. Armstrong, H. Mosegaard, H. Jensen, I.M. Gibb, H. Fraser, *et al*. "Variation in the abundance of sandeels Ammodytes marinus off southeast Scotland: an evaluation of area-closure fisheries management and stock abundance assessment methods." *ICES Journal of Marine Science*. 63. (2006): 1530-1550.
15. Gerlotto, F., and P. Freon. "Some elements on vertical avoidance of fish schools to a vessel during acoustic surveys." *Fisheries Research*. 14.4 (1992): 251-259.
16. Gerlotto, F., M. Soria, and P. Fréon. "From two dimensions to three: the use of multibeam sonar for a new approach in fisheries acoustics." *Can. J. Fish. Aquat. Sci*. 56. (1999): 6-12.
17. Guillard, J., D. Geredeaux, G. Brun, and R. Chappaz. "The use of geostatistics to analyse data from an echo-integration survey of fish stock in Lake Sainte-Croix." *Fisheries Research*. 13.4 (1992): 395-406.
18. Halfsteinsson, M.T, and O.A Misund. "Recording the migration behaviour of fish schools by multi-beam sonar during conventional acoustic surveys." *ICES Journal of Marine Science*. 52.6 (1995): 915-924.
19. Harbitz, A., E. Ona, and M. Pennington. "The use of an adaptive acoustic-survey design to estimate the abundance of highly skewed fish populations." *ICES Journal of Marine Science*. 66. (2009): 1349-1354.
20. Hassel, A., T. Knutsen, J. Dalen, K. Skaar, S. Løkkeborg, O.A. Misund, Ø. Østensen, M. Fonn, et al. "Influence of seismic shooting on the lesser sandeel (*Ammodytes marinus*)." *ICES Jorunal of Marine Science*. 61.7 (2004): 1165-1173.
21. Hjelmervik, K.T, and G.H. Sandmark. "In ocean evaluation of low frequency active sonar systems." *Acoustics 08 Paris*. (2008): 2839-2843.
22. Holland, G.J., I.M. Greenstreet, H.M. Fraser, and M.R. Robertson. "Identifying sandeel *Ammodytes marinus* sediment habitat preferences in the marine environment." *Marine Ecology Progress Series*. 303. (2005): 260-282.
23. ICES. "Report of the ICES Advisory Commitee 2010". *ICES Advice, 2010*. Book 6 North Sea. (2010): 309 pp.

24. Jensen, H., P. J Wright, and P. Munk. "Vertical distribution of pre-settled sandeel (*Ammodytes marinus*) in the North Sea in relation to size and environmental variables." *ICES Journal of Marine Science*. 60. (2003): 1342-1351.
25. Johannessen, T. "Havets ressurser og miljø 2009" *Fisken og Havet, Inistute of Marine Research. Bergen.* 1. (2009): 133-134
26. Johnsen, E, R. Pedersen, and Ona E. "Size-dependent frequency response of sandeel schools."*ICES Journal of Marine Science*. 66. (2009): 1100-1105.
27. Korneliussen, R J, and E Ona. "An operational system for processing and visualizing multi-frequency acoustic data." *ICES Journal of Marine Science*. 159. (2002): 293-313.
28. Korneliussen, R. J., Eliassen, I. K., Heggenlund, Y., Patel, R., Godø, O. R., Giertsen, C., Patel, D., et al. 2006. The large scale survey system—LSSS, a new post processing system for multifrequency echo sounder data. (2006) 6pp.
29. Korneliussen, R.J., N. Diner, E. Ona, L. Berger, and P.G Fernandes. "Proposals for the collection of multifrequency acoustic data." *ICES Journal of Marine Science*. 65. (2008): 982-994.
30. Kubilius, R. "Target strength and tilt angle distribution of lesser sandeel (Ammodytes marinus"). MSc thesis. Ecology and Environmental Sciences, Klapeida University. (2009): 64 pp.
31. Kubilius, R., and E. Ona. "Target strength and tilt-angle distribution of the lesser sandeel (*Ammodytes marinus*)." *ICES Journal of Marine Science*. 69.6 (2012): 1099-1107.
32. Løkkeborg, S., E. Ona, A. Vold, and A. Salthaug. "Sounds from seismic air guns: gear- and speciesspecific effects on catch rates and fish distribution." *Can. J. Fish. Aquat. Sc*. 69. (2012): 1278-1291.
33. Macer, C.T. "Sandeels (Ammodytidae) in the south-western North Sea: their biology and fishery." *MAFF Fish. Investig. Londn*. 2.24 (1966): 55 pp.
34. Mackinson, S, K Turner, D Rightin, and J.D Metcalge. "Using acoustics to investigate changes in efficiency of a sandeel dredge." *Fisheries Research*. 71. (2005): 357-363.
35. MacLennan, D.N, P.G Fernandes, and J. Dalen. "A consistent approach to definitions and symbols in fisheries acoustics." *ICES Journal of Marine Science*. 59. (2002): 365-369.

36. Misund, O.A. "Sonar observations of schooling herring: school dimensions, swimming behaviour, and avoidance of vessel and purse seine." *Rapp. P.-v. Reun. Cons. int. Explor. Mer*. 189. (1990): 135-146.
37. Misund, O.A, A. Aglen, and E. Frønæs. "Mapping the shape, size, and density of fish schools by echo integration and a high-resolution sonar." *ICES J. mar. Sci.* 52. (1995): 11-20.
38. Misund, O.A., and J. Coetzee. "Recording fish schools by multi-beam sonar: potential for validating and supplementing echo integration recordings of schooling fish." *Fisheries Research*. 47 . (2000): 149-159
39. Mjanger, H., Hestenes, K., Olsen, E., Svendsen, B. V., and Wenneck,. D. L. "Manual for Sampling of Fish and Crustaceans", *version 1.0. Institute of Marine Research, Bergen, Norway*. (200): 165 pp.
40. Mohammed, Z. "Acoustic identification of sandeel (Ammodytes marinus) using multi-frequency methods". MSc thesis, Department of Biology, University of Bergen. (2006): 68 pp
41. Nakken, O., and K Olsen. "Target strength measurements of fish." *Hydro-acoustics in fisheries research*. 170. (1977): 52-69
42. Ona, E. "Mengdemåling av tobis og planktonovevåkning i Nordsjøen i april/mai 2006." *Institute of Marine Research. Survey Report* (2007): 14pp.
43. Ona, E. "Erfaringer fra NFR prosjektet: "Mengdemålingsmetodikk for tobis"." SMASSC. Institute of Marine Research. Bergen. (2010): 75 pp.
44. Petitgas, P., D. Reid, P. Carerra, M. Iglesias, S. Georgakarakos, B. Liorzou, and J. Masse. "On the relation between schools, clusters of schools, and abundance in pelagic fish stocks." ICES Journal of Marine Science. 58. (2001): 1150-1160.
45. Petitgas, P., J. Masse, P. Beillois, E. Lebarbier, and A Le Cann. "Sampling variance of species identification in fisheries-acoustic surveys based on automated procedures associating acoustic images." *ICES Journal of Marine Science*. 60. (2003): 437-445.
46. Pitcher, T.J, A.E Magurran, and J.I Edwards. "Schooling mackerel and herring choose neighbours of similar size." *Marine Biology*. 86. (1985): 319-322.
47. Pitcher, T., O.A Misund, A. Fernö, B. Totland, and V. Melle. "Adaptive behaviour of herring schools in the Norwegian Sea as revealed by high-resolution sonar." *ICES Journal of Marine Science*. 53. (1996): 449-452.
48. Rasband, W.S., T. Ferreira." ImageJ User Guide." *U. S. National Institutes of Health, Bethesda, Maryland, USA*. 1.45 (2011): 167 pp.

49. Redwood, W.N., C.H. Thompson, and J.M. Jech. "In situ acoustic estimates of the swimbladder volume of Atlantic herring (*Clupea harengus*)." *ICES Journal of Marine Science*. 61. (2004): 323-337.
50. Simmonds, J.E., N.J. Williamson, F. Gerlotto, and A. Aglen. "Survey Design and Analyses Procedures: a comprehensive review of good practise." *ICES Fish Capture Committee Theme Session Application and Analyses of Acoustic Methods*. 54. (1991): 94 pp.
51. Simmonds E. J., and D.N. MacLennan., "Fisheries Acoustics: Theory and Practice". *Second edition. Blackwell Publishing, Oxford, England*. (2005): 437 pp.
52. Simrad, "Simrad SH90 Product decription." *Kongsberg Maritime AS*. Ver:A. (2009): 5-38.
53. Soria, M, P. Fréon, and F. Gerlotto., "Analysis of vessel influence on spatial behaviour of fish schools using a multi-beam sonar and consequences for biomass estimates by echo-sounder." *ICES Journal of Marine Science*. 53. (1996): 453-458.
54. Thompson, S.K., "Adaptive Cluster Sampling." *Journal of the American Statistical Association*. 85.412 (1990): 1050-1059.
55. Winslade, P., "Behavioural studies on the lesser sandeel (*Ammodytes marinus*)." *Journal of Fish Biology*. 6.5 (1974): 565-599.